Embedding Binary Metal Chalcogenide Nano Partials In Carbon Matrix For Economically Viable Lithium-Ion Batteries Anode

By

Muhammad Ali

School of Chemical and Materials Engineering

National University of Sciences and Technology

2021

Embedding Binary Metal Chalcogenide Nano partials In Carbon Matrix For Economically Viable Lithium-ion Batteries Anode

Name: Muhammad Ali

Reg.No: 273438

This thesis is submitted as a partial fulfillment of the requirements for the degree of

MS in Materials and Surface Engineering

Supervisor Name: Dr. Zeeshan Ali

School of Chemical and Materials Engineering (SCME)

National University of Sciences and Technology (NUST)

H-12 Islamabad, Pakistan

December 2021

DEDICATION

To my Parents, who supported me in every aspect of life and my siblings.

Acknowledgments

Firstly, all praise Allah Almighty, who has provided me with appropriate skills, guidance, strength, perseverance, power of the mind, and uncountable blessings that allowed me to complete this study.

I want to dedicate this study to my beloved parents, who have always acted a source of inspiration for me and gave me hope again and again when it was required. I would also like to dedicate this thesis to my supervisor Dr. Zeeshan Ali who allowed me to be part of his research group at SCME NUST. The blend of his patience, persistence, guidance, and motivation made me accomplish my research aims.

I would also like to thank Dr. Ghulam Ali, Dr. Aftab Akram, and Dr. Sofia Javed for their unmatchable suspport during my research.

Abstract

Excessive use of fossil fuels is negatively impacting the global economy. Using fossil fuels as an energy source is also affecting the environment. Hence, there is a need to replace fossil fuels with environmentally friendly and cost-effective materials. Lithium Batteries are a good candidate for this purpose. The main issue with Lithium batteries is that they are expensive, and the electrode material used in these are not environment friendly such as (nickel, Cobalt, etc.). Because of their remarkable electrochemical properties, multiple metal selenides (MMSs) have drawn the interest of scientists as potential electrode materials for energy storage devices. When compared to single-metal selenides, they exhibit higher intrinsic conductivities and more redox sites. However, the cost of precursor, limited cycle stability, and low-rate capabilities are still problems for researchers. The cost of precursors can be tackled by selecting cheap elemental combinations such as Aluminum and Copper coupled with carbon matrix, which increases intrinsic conductivity, rate capability, and long-term cyclic stability. A facile methodology is prepared to improve intrinsic conductivity, a hierarchically porous multiple metal selenide (Al-Cu-Se termed as ACSe) nanomaterials. The porous structure, embedded nanoparticles, combination with carbon matrix, and good conductivity result in extraordinary electrochemical performance. When employed in lithium metal batteries as anode material, as prepared ACSe showed good rate capability (532 mAh g^{-1} at 0.1 A g^{-1} and 400 mAh g^{-1} at 8 A g^{-1}), sufficient cyclic stability (350 mAh g^{-1} after 2000 cycles at 1 A g^{-1}), and high specific capacity (633.6 mAh g^{-1} at 0.1 A g^{-1} and 492.1 mAh g^{-1} at 4 A g^{-1}). This novel combination of Aluminum Copper Selenide with nanochannels can be a good candidate for following generation energy storage devices.

Table of Contents

List of Figures

List of Tables

Chapter 1

1.1 Introduction

The world is moving away from the utilization of fossil fuels because of their adverse environmental effect and great contribution towards global warming [1]. Moreover, fossil fuels have limited resources as compared to increasing energy demand [2]. Carbon dioxide is the most influencing GHG (Green House Gas) which is mainly produced by the burning of fossil fuels. The abundant uses of the conventional resources cause the increase of such gases that cause the increase in overall temperature of the earth atmosphere, such phenomenon known as global warming. The global warming cause 0.13 C rise in temperature per decade. The study estimate that the world's average global temperature will experience a rise of 1.5 °C in the next ten decades [3]. In February 2007, the Intergovernmental Panel on Climate Change (IPCC) published a study on the rise in global concentrations of methane, nitrous oxide and carbon dioxide due to fossil fuel burning and other pollution-causing activities [4]. Another problem with fossil fuel use is its rapid degradation, causing it to disappear. It takes millions of years for fossil fuels to develop, and they are finite. In order to meet the need for affordable energy with the urgent problem of climate change, there is a need to implement new policies that ensure the uses of renewable energy resources other than the conventional fossil fuels to have sustainable solutions [5]. Hence the world is looking for new renewable energy resources, for example, solar and wind energy. The main issue with these energy resources is that they are intermittent, due to which energy form these resources is not available for sufficiently long period [6]. To store this energy, we need a storage system that continuously provides energy. The need for massive energy storage systems is continuously increasing, requiring low-cost and renewable storage devices with maintainable performance. At present, the researchers' primary objective is to search and develop advanced techniques to improve the energy utilization ratio. Scientists struggle to produce efficient methods: Firstly, to generate energy directly from renewable sources such as the direct conversion of solar power, oxygen reduction reaction, and water splitting, and secondly, efforts are being carried out to store energy from such resources. Moreover, researchers are trying to develop environmentally friendly devices, cheap and have extraordinary performance. To overcome these

problems, a considerable effort has been made in making energy storage devices that have high performance, such as batteries and supercapacitors.

1.2 Energy Storage devices

Energy can be store by various methods. The many methods of energy storage can be classified into five major technology categories.

- Batteries
- Thermal
- Mechanical
- Pumped hydro
- Hydrogen

Batteries are the most common, oldest, and widely available energy storage method. They are made up of one or more cells having a cathode (+ive terminal) and an anode (-ive terminal). A variety of chemistries are used in batteries. Li-ion and lead acid batteries are the most well-known and commonly used batteries in portable electronic devices and automobiles [7]. Other solid battery types include nickel-cadmium[8], sodium-sulphur [9], and zinc-air [10] etc. Flow batteries using liquid electrolyte solutions are another group, which includes vanadium redox[11] and iron-chromium[12] and zinc-bromine[13] etc chemistries. Although not technically a battery, supercapacitors can be classified as an electrochemical technology due to their applicability to sub-minute level response. There are two basic phenomena used for electrochemical energy storage. One is faradic ion exchange, and the other is electrostatic charge accumulation on the surface of the electrode [14]. In faradic ion exchange charge transfer during discharge of a Lithium-ion battery are shown schematically in Fig 1-1 the cell consists of three main parts such as anode (copper current collector), cathode (aluminum current collector), and a separator. Both the electrodes and separators are porous The electrode is made up of active material, a polymer binder, conductive filler, and an electrolyte. Lithium hexafluorophosphate ($LiPF_6$)[15] is used as the electrolyte in a solution of propylene carbonate, ethylene carbonate, and dimethyl carbonate. A polymer matrix and a liquid electrolyte comprise the porous separator. Fig 1-1 also illustrates a hypothetical lithium diffusion model in anode and cathode active materials during battery charging. Li ions travel from the cathode to the anode during charging and back from the anode to the cathode during

discharging. Li+ may be stored in a variety of methods, such as by intercalation, alloying, and conversion.

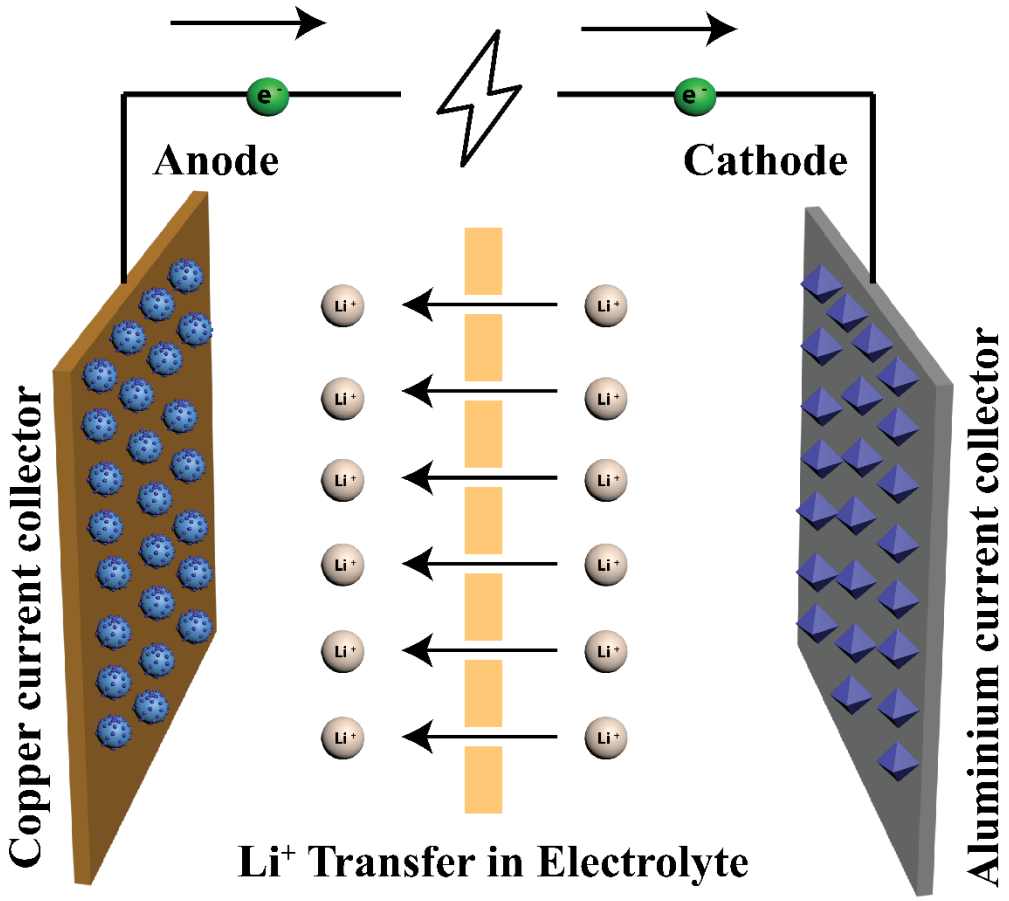

Figure 1-1 Mechanism of Li^+ batteries

Thermal storage involves the absorption and release of heat as a result of a chemical interaction between a solid, liquid, or gas. There may be a shift in the condition of the medium, such as liquid to gas, solid to liquid, or vice versa. Molten salt and liquid air storage are two examples of such energy storage systems. The molten salt alternative with concentrated solar power is the most economically viable heat storage option; nevertheless, this and other heat storage systems may be constrained by the need for massive underground storage caverns. [16].

Mechanical energy storage devices, which rely on rotational or gravitational forces to store energy, are possibly the most basic. However, feasibility in today's grid applications requires modern technology. Flywheels [17] and compressed air systems[18], are main types of mechanical energy storage devices whereas

gravitational energy is a relatively new technology with a variety of applications under development.

Energy storage via pumped hydro systems based on large water reservoirs has been widely deployed during the last century, becoming the most popular type of utility-scale storage worldwide [19]. These systems only work when water is being cycled between two varying levels. Potential energy is stored in water which is at higher level and this energy is then converted in useful work.

Hydrogen energy storage, require electricity for electrolysis in result hydrogen is produce which is then store in tanks. This energy storges method is still in its early stages [20]. From there, it can be used for different purposes such as transportation, industry, or residential as a supplement or alternative for gas. Intermitted energy conversion means necessitate the integration of energy storage devices (e.g., batteries) [21]. The main advantage of these energy storage devices over others is that they have a high energy density, however, limited cycle life and inability to quickly charging/discharging poses great hindrance of this system. Development of electrodes with greater conductivity and higher storage capacity may prove to be a viable solution to address these issues.

Supercapacitors are highly efficient energy storage devices also known as ultracapacitors. Supercapacitors have several features such as fast processing, rapid charging/discharging, and long-term cycle stability [22].Supercapacitor is a device that stores electric energy in the form of an electric field produced on the electrode's surface. There are four main parts of the capacitor in which there are two electrodes an electrolyte and a dielectric. Its ability to store charge is known as capacitance. There are three types of supercapacitors

- Electrochemical double-layer capacitor (EDLC)
- Pseudo capacitor
- Hybrid capacitor

In EDLC, behavior charges accumulate on the surface of the electrode in response to the applied voltage. The figure shows the EDLC behavior of a capacitor. In this type of behavior, Area and distance between the parallel plates play a crucial role because high surface area makes more contact between electrolyte and active material, making it more possible to store more charge on the surface of the electrode.

In this type of supercapacitor, there is no electrochemical reaction (redox reaction). This type of behavior is generally shown by carbon-based materials such as Graphene, CNTs, MWCNTs, Activated Carbon, etc.

In pseudo capacitors, redox reactions are involved. There are three basic reactions such as

- Insertion
- Conversion
- Alloying

The selection of material requires which can exhibit one of above mention reactions. There is a large variety of materials that show this type of behavior, such as metal chalcogenides, metal oxides, and some composites, etc. Such energy storage devices also have some disadvantages, such as having low energy density compared to batteries that use faradic reactions for charge storage. [23]

Hybrid supercapacitors are those capacitors that show both behavior, i-e, EDLC, and pseudo capacitor. It contains two electrodes separated by a semipermeable film which acts as a separator to isolate both electrodes from electrical contact. An electrolyte solution is impregnated on the electrodes and separator, allowing ions to flow between electrodes, and stopping electrons from discharging the cell. A comparative systematic diagram between EDLC, Pseudo, and Hybrid supercapacitor is shown.

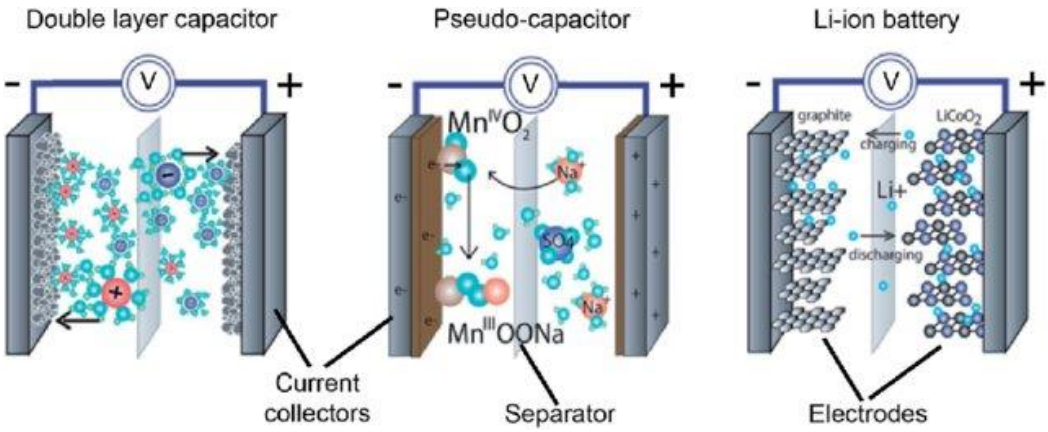

Figure 1-2 Comparison between EDLC capacitor, pseudo capacitor, and Hybrid (lithium-ion battery)

1.2.1 Batteries

Demand for energy storage media increases with the fast development of renewable energy conversion devices. Different types of batteries are being used for energy storage applications. There are two main categories of batteries.

I. Physical batteries
II. Chemical batteries

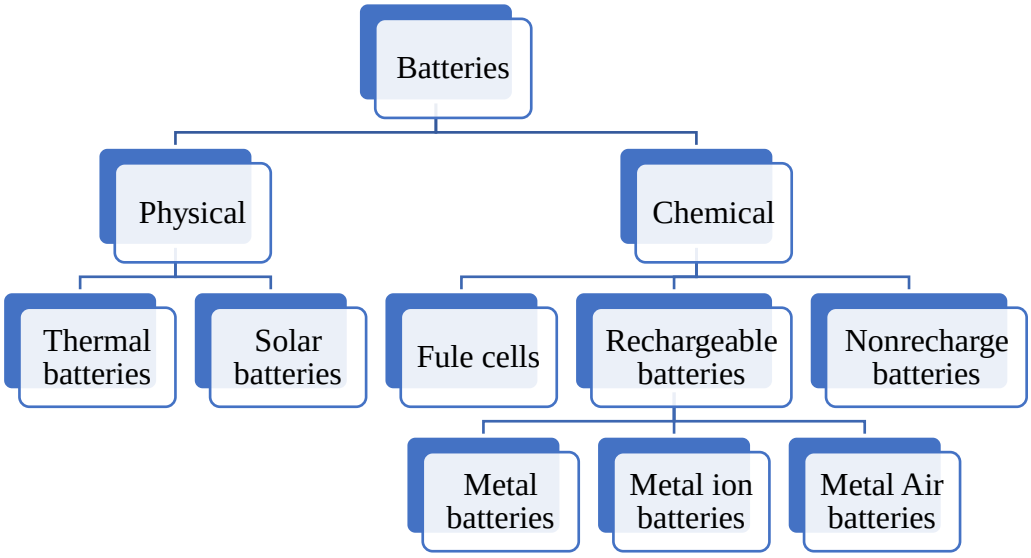

Figure 1-3 Classification of batteries

1.2.1.1 Physical Batteries

Physical batteries are those batteries that generally produce electric energy by physical change. There are further two types of physical batteries: thermal and solar batteries. Thermal batteries store electric energy by converting heat into chemical energy and delivering electricity during discharge. They can be used to utilize waste heat in the plant where fossil fuels are burnt and nuclear plants. The performance of physical batteries depends on the environment, which hinders their performance. Solar batteries directly convert the energy of light into electricity.

1.2.1.2 Chemical batteries

Chemical batteries are also known as electrochemical cells. In these types of batteries, there are redox reactions on electrodes. There are three further types of chemical batteries: fuel cells, rechargeable batteries, and non-rechargeable batteries.

Fuel cells generate energy using several chemical redox reactions between a fuel and oxidizing agent, usually oxygen. Generally, fuel cells consist of three components. A schematic diagram for working a fuel cell is shown in figure 1.3 Fuel cells are classified into different

key component in fuel cell operation; it transfers the ions from one electrode to other generated during a chemical redox reaction. Potassium hydroxide, acids, and a few salt carbonates are used in a fuel cell as an electrolyte. The most common types of fuel cells are listed below:

i. Alkaline fuel cell

ii. Polymer exchange fuel cell

iii. Solid oxide fuel cell

iv. Phosphoric acid fuel cell

v. Molten carbonate fuel cell

The alkaline fuel cell was the first commercially viable fuel cell device, allowing to produce electricity from hydrogen. The alkaline cell was suited for space applications due to its lack of moving components and high energy conversion efficiency. Alkaline fuel cells employ a solution of potassium hydroxide in water as the electrolyte, typically at a concentration of around 30%. The electrodes are composed of two layers: an electrocatalyst layer and a hydrophobic layer. Kivisaari et al. [24] and De Geeter [25] describe a dry manufacturing technique. In this technique organic mixture consisting of carbon black, catalyst and PTFE was rolled at room temperature to generate a self-supporting sheet. A porous organic layer is made through rolling at room temperature. This layer prevents leakage of electrolyte into reactant gas. It also allow gas diffusion to the reaction site. After that, these two layers

are sandwiched together onto a conductive metal mesh. Sintering is used to finish the process. The overall thickness of the electrodes is in the range of 0.2–0.5mm.

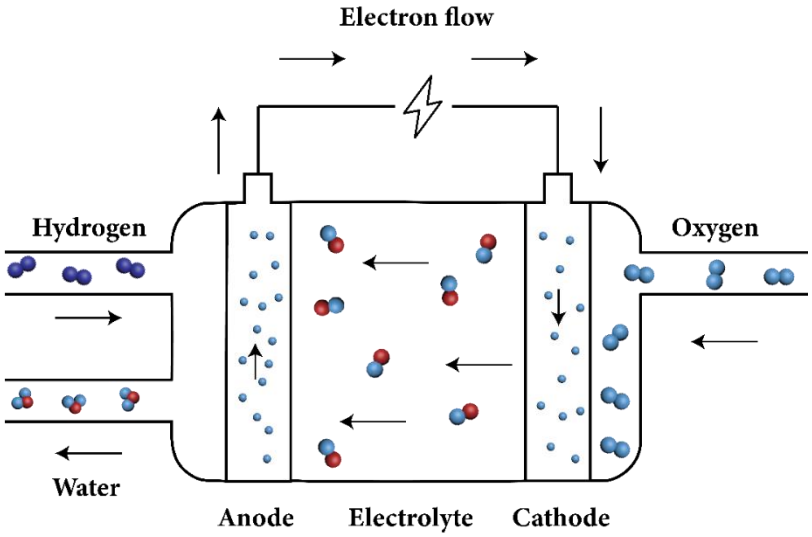

Figure 1-4 Alkaline fuel cell composition

The proton exchange membrane fuel cell (PEMFC) consists of an electrolyte made up of water-based acidic polymer membrane platinum-based electrodes. Protons moves towards cathode side while electron travels through an external circuit and provide energy.

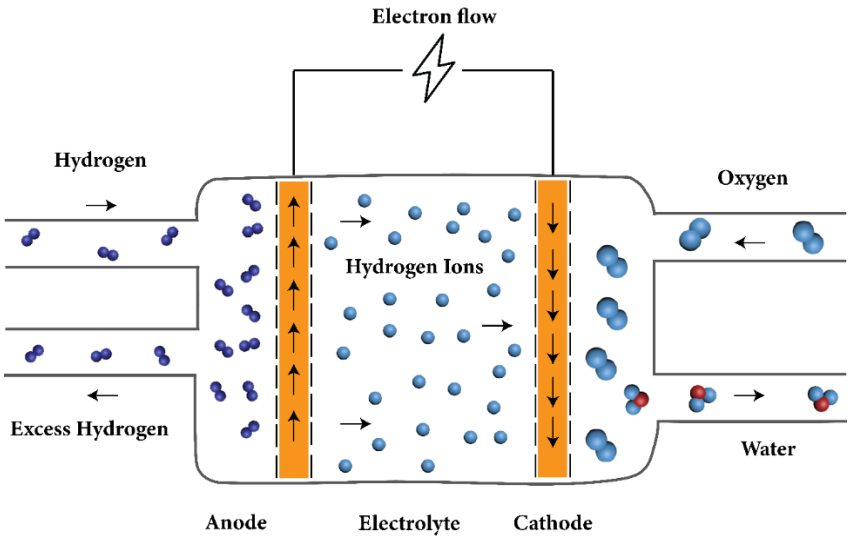

Figure 1-5 working of Proton exchange membrane fuel cell

Solid oxide fuel cells (SOFCs) use an electrolyte made of a hard, ceramic mixture of metal oxides (for example, calcium or zirconium). The efficiency of these fuel cells is roughly about 60%. The operating temperature is around 1,000 °C (1,800 °F). The cells can produce up to 100 kW. Because of the high temperature, a reformer is required for these cells, which extract hydrogen from the fuel. Waste heat may be recovered to provide additional energy. On the other hand, the high working temperature limits the applications of SOFC units, which are typically relatively large. While solid electrolytes are impenetrable to leakage, they are brittle and prone to fracture [26].

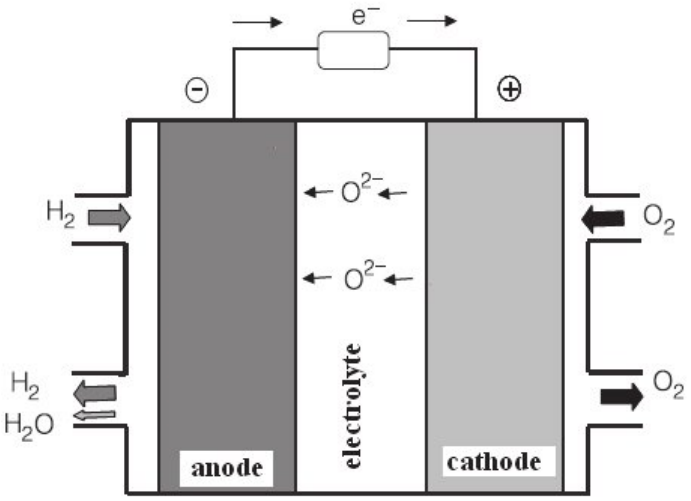

Figure 1-6 Working of solid oxide fuel cell

Phosphoric acid serves as the electrolyte in phosphoric acid fuel cells (PAFC). The efficiency ranges from 40 to 80 percent. The working temperature is between 150 and 200 °C (300 and 400 °F). The greatest commercially available phosphoric acid cell output is 200 kW, and 11 MW units have been tested. P A F Cs have a carbon monoxide content of around 1.5 percent, allowing them to run on a broader spectrum of fuels. Prior to usage, sulfur must be eliminated from gasoline. Platinum electrode-catalysts are necessary, as are internal components that are resistant to the acid's corrosive nature.

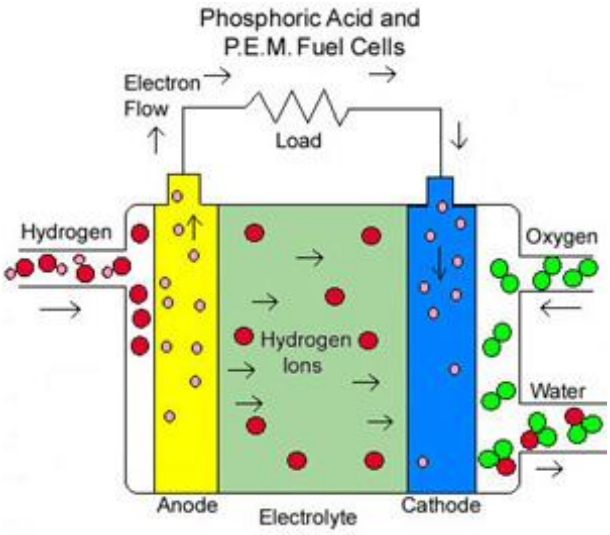

Figure 1-7 Working of Phosphoric Acid

Molten carbonate fuel cells (MCFC) use high-temperature salt carbonates as its electrolyte (CO_3). The efficiency ranges between 60 and 80 percent. The working temperature is around 650°C (1200°F) Units of up to 2 MW have been built, while designs for units of up to 100 MW exist. The high temperature prevents carbon monoxide poisoning, and waste heat may be recovered to produce additional energy. Their nickel electrode-catalysts cost less than platinum electrode-catalysts. M C F Cs, due to their high temperature, may be too hot for domestic usage. Carbon dioxide infusion is necessary to compensate for electrolyte carbonate ion depletion. [27].

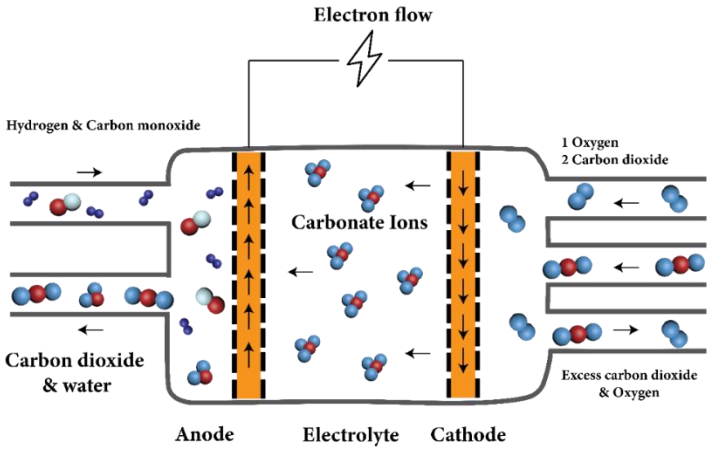

Figure 1-8 Working of Molten carbonate fuel cells

Non-rechargeable batteries are also known as primary batteries. These are primarily used in portable devices. The key feature of primary batteries is one cycle of a lifetime. It is only a one-time chargeable device. These batteries are further classified

into different types because of the electrolyte being used in them. These batteries use both types of electrolytes, i.e., aqueous, and non-aqueous.

Secondary batteries are referred to as rechargeable batteries. They can be used in electric vehicles, solar cell operations, portable devices (mobile phones, laptops), etc. These devices can be further classified based on electrode material used, such as lead batteries, metal-ion batteries, etc.

Chapter 2
Literature Review

2.1 Literature Review

Lithium being the lightest element results in batteries of highest voltage and greatest energy density in all metals. The era of lithium batteries began when Harris published the first work about lithium batteries in 1958 [28]. His work eventually led to the commercialization and development of primary lithium cells of different varieties in the 1970s. The most crucial system was lithium-polycarbonic monofluoride[29], lithium iodide [30], lithium sulfur-dioxide [31], lithium manganese dioxide [32], lithium sulfuryl chloride [33] Numerous efforts were made in the 1980s to produce rechargeable lithium batteries, but there were many hurdles and difficulties in developing rechargeable lithium batteries. The particles and flame are problems related to the high reactivity of metallic lithium, especially in the open environment when the electrodeposited lithium rapidly reacts with the electrolytic solution. In early research aquas based electrolyte is used for lithium batteries. Lithium metal anode is undoubtedly best anode for lithium batteries, but they are highly reactive towards water. Due to this, the use of the non-aqueous electrolyte in the primary and secondary lithium batteries increases, which is less conductive than the aqueous electrolytes. To improve the Li-solution interface's safety and utility, the lithium electrode's reaction was extensively studied. The different strategies were implied to advance the reactivity of the lithium-solution interface.[34].

In the late 1970s and 1980s, the first rechargeable lithium batteries were introduced by Exxon Ldt. and Moli Energy Ldt. [35]that used the lithium compounds as positive electrodes. These systems operated on very low voltage, nearly 2 volts [36],

In early research scientist reviewed the synthesis and characteristics of various compounds which store charge by intercalation process. The most significant compunds that found their way into the batteries were MnO_2, V_2O_5, and V_6O_{13}. All these devices employed a metallic lithium anode as their cathode. The safety concerns restricted the commercial implementation of rechargeable lithium metallic anodes batteries [37].

Lithium metal can be a good candidate for anode material in lithium batteries because it does not have any inactive material and can act as ultimate source of Li ions.

Main problem with Lithium metal anode is uncontrolled growth of lithium dendrites during cycling. These dendrites can penetrate through electrolyte and separator and cause a short circuit. Inspired by Hagenmuller's [38] 1973 research on Na_xCoO_2, Goodenough et al. [39] substituted Li for Na and patented $LiCoO_2$ as a novel cathode (3.9 V vs. Li^+/Li). Li-ion batteries have high energy density, little self-discharge and no memory effect (excluding LFP cells [40]) [41]. Cells may be made to emphasize power or energy density. They contain volatile electrolytes and may cause explosions and flames if damaged or inappropriately charged.

Akira Yoshino and his colleagues developed a prototype of Li-ion battery in 1985.This prototype was based on the 1970s-1980s research of John Goodenough, M. Stanley Whittingham, Rachid Yazami, and Koichi Mizushima.Yoshio Nishi led a Sony and Asahi Kasei team that developed a commercial Li-ion battery in 1991.

Among numerous materials, transition metal chalcogenides (TMCs) have gained attention due to their high theoretical specific capacity for usage in a variety of energy applications, including batteries.

. These systems include (Li_xMO_2) whereas M is Co, Ni, or Mn [37, 42]. In that era, the technique of cycling lithium ions between two insertion electrodes was tested in the laboratory, which caused the elimination of the metallic lithium anode [43, 44]. There are three main parts in Li-ion batteries cathode, anode, and electrolyte. On cathode materials, scientists have already put a lot of effort into it. For example, the first cathode $LiCoO_2$ for Li-ion batteries prepared by Dr. John Goodenough in 1973[37] A lot of work has been done since then on enhanced battery storage devices that work on introducing lithium ions to host materials that act as both electrodes. Finding the suitable material to accommodate lithium ions as battery negative requires a lot of effort. There four main parts of li-ion battery anode, cathode, separator, and electrolyte.

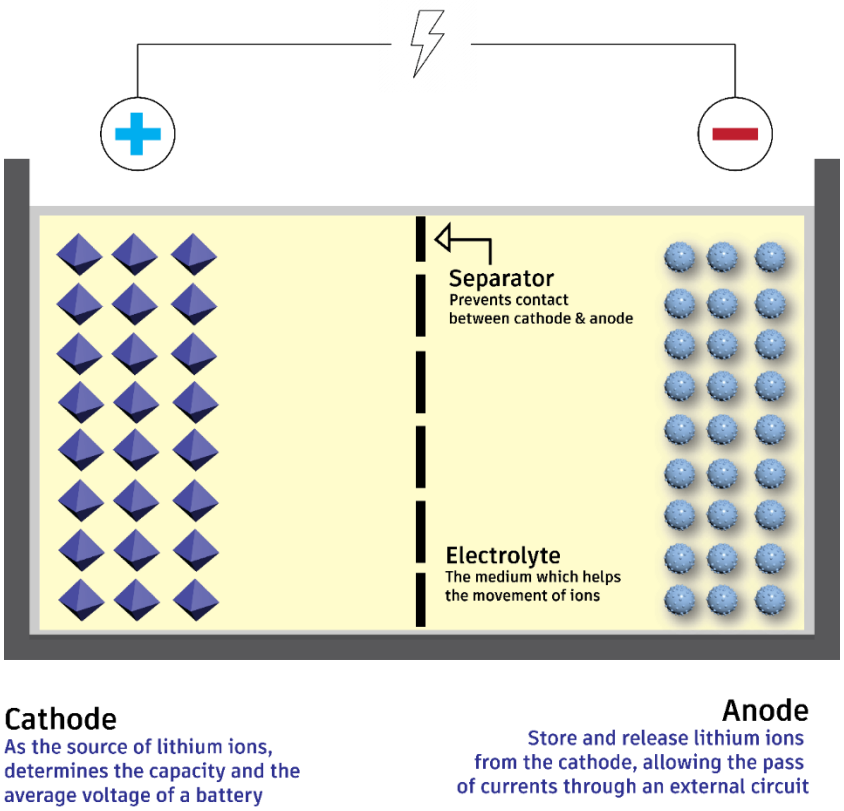

Figure 2-1 The Four Components of Li-ion Battery

Lithium-ion batteries create power by chemical reactions between the lithium atoms. Therefore lithium is used in batteries, and the space allocated for lithium is referred to as the "cathode". Due of lithium's reactivity in its elemental state, a lithium compound is used as the cathode. The phrase "active material" refers to the substance that interferes with the actual battery's electrode response. In other words, a lithium compound serves as the active ingredient in the cathode of a lithium-ion battery.

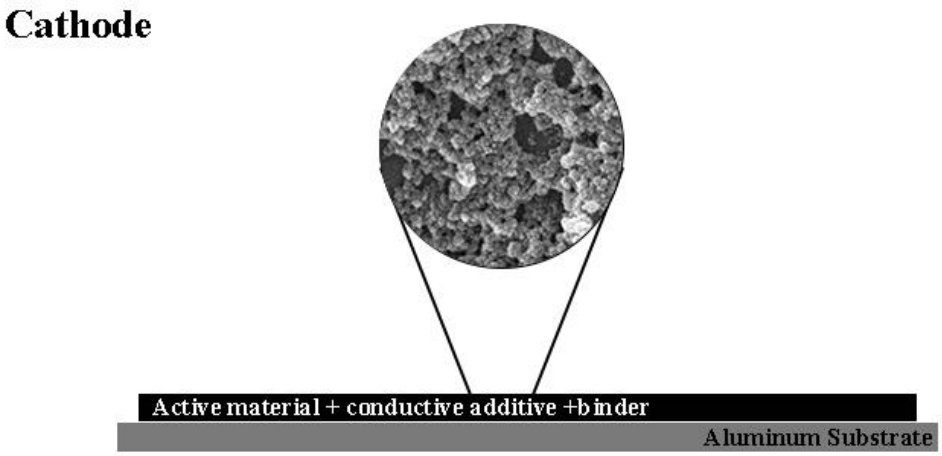

Figure 2-2 schematic diagram of cathode used in li-ion battery

A thin metal foil is covered with a composite consisting of active material, a conductive additive, and a binder to adhere to the cathode. The active material comprises lithium ions. The conductive additive promotes conductivity. The binder acts as an adhesive, ensuring that the active material and conductive additive suitably adhere to the aluminum substrate.

The cathode is crucial as it determines the battery's features since the active material type of the cathode influences the battery's capacity and voltage. The higher the voltage, the more lithium in the battery, and the more significant the potential difference between the cathode and anode. While the potential difference between anode and cathode varies greatly depending on their kind, the potential difference between cathode and anode is often rather significant. As a result, the cathode is vital in deciding the battery's voltage.

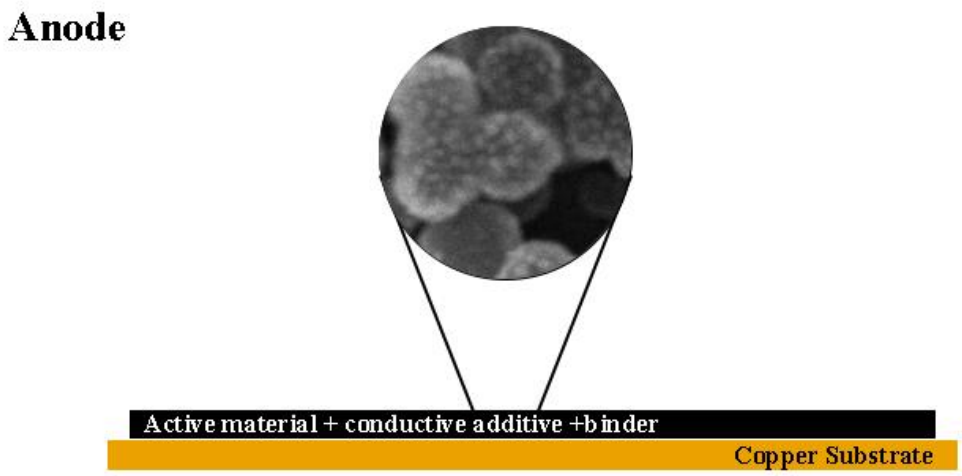

Figure 2-3 schematic diagram of Anode used in li-ion battery

Assume that cathode represents a home, anode represents a restaurant, and lithium-ion represents a customer. Charging happens when a customer (lithium-ion) leaves its house (cathode) and travels to a restaurant (anode) to eat and discharging occurs after the customer has finished eating and returns home. However, what if the restaurant is unable to accommodate everyone? The restaurant increased the number of seats on the outdoor patio, but what if the chairs are too close to the busy road? In that instance, the customer is unable to eat at the restaurant, the restaurant is unable to sell food, and the restaurant's outside patio may be jeopardized.

As a result, without a secure location for lithium-ion, we cannot ensure the cathode's capacity or power. However, with proper anode design, we may get a higher capacity and longer life for the battery.

Battery life may be decrease by charging and discharging a lithium-ion battery continually. The anode structure breaks down due to deterioration of the anode which absorbs lithium-ion. No matter how durable a product is, it ages and degrades with time.

Batteries are the same. Anode size changes are not unsafe because they are natural. Anode volume change also influences capacity. When developing a battery, we consider structural modifications. We can't forecast size fluctuations and build enough rooms if we employ materials that grow rapidly. Using non-expandable materials, we can create enough gaps to increase battery capacity.

Fig 2-3 shows that the anode substrate (copper) is coated with active material, just like the cathode. The anode's active material lets current pass via the external circuit while allowing the cathode's reversible absorption/emission of lithium ions. The lithium ions are stored in the anode when the battery is charged. Lithium ions flow naturally to the cathode via the electrolyte (discharge state) when the conducting wire connects the cathode. The separated electrons from the lithium ions move over the wire, creating energy.

Afterward, there has been a tremendous amount of work done covering every aspect of the lithium-ion batteries, technical advancement, battery design-related work, from manufacturing to application.

2.1.1 Anode Materials for Li-ion Batteries

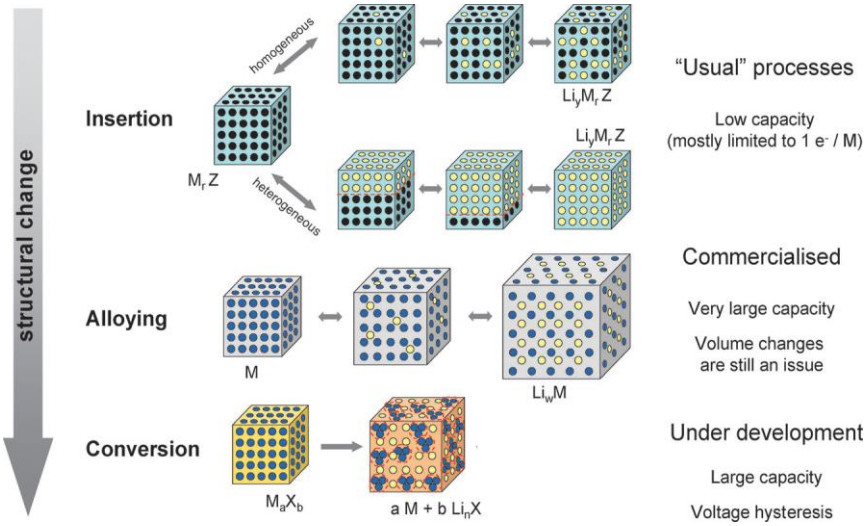

Figure 2-4 Different types of process involved in (dis)charging

For lithium-ion batteries, the ideal anode materials should be the one that exhibits all the properties like low potential against cathode, possesses cost-effectiveness, shows high reversible gravimetric and volumetric capacity, exhibits extended cycle life of charging and discharging process, shows high-rate capability, and withstands mechanical abuse. Pure lithium is the best anode material based on only specific capacity because it does not have any inactive material that is dead weight. But it has severe safety concerns due to the electroplating of the dendritic lithium during the charging process [45]. These dendrites can penetrate through electrolyte and separator and cause a short circuit. Hence, several other anode materials have been explored and are being employed. These anodes can be categorized into three types depending upon lithiation and de-lithiation processes (i.e., intercalation, alloying and conversion). Fig. shows three types of processes.

2.1.2 Intercalation Type Anodes

There are different types of anodes in which the lithium is stored in the material through intercalation and de-intercalation. Carbonaceous material show intercalation behavior they have good working potential, good safety and are low cost [46] but common issues with these type of material they have high voltage hysteresis and have high irreversible capacity [47, 48]. Titanium oxides also show this type of behaviour they are extremely safe, low cost, long cycle life but they have very low capacity and low energy density [49].

For lithium-ion batteries, the best anode material is carbon-based material with different morphologies due to their unique features such as stability in different environments like electrochemical, chemical, and thermal environments, low cost, abundant presence in the earth, and good lithium insertion and reinsertion reversibility [23, 50, 51]. These features are critical when considering the charged electrode material, both types, either lithiated anodes or delighted cathodes, at a high temperature which will highly react with the non-aqueous electrolytes. At room temperature, a side reaction can also occur mainly the lithium salt LiPF6 will react with the moisture and form HF. The formation of HF causes the dissolution temperature of any type of transition metal in the electrodes that cause the active material surface erosion that leads to failure or capacity fading upon charging and discharging cycles. In lithium-ion batteries, the carbon-based material used as an

active anode is classified into two types based on carbon atom stacking and crystallinity [52, 53] The one is SOFT carbon in which the crystallites are stacked in almost the same direction that is also known as Graphitizable carbon. The second one is HARD carbon in which the crystallite has no order that also known as non-graphitizable carbon [54-56].

Soft carbon is an excellent anode material for lithium-ion batteries, but it has several shortcomings, such as high voltage hysteresis in the delithiation process and low capacity, limiting its application in next-generation lithium-ion batteries. Hard carbon is an alternative to soft carbon that has a very high reversible capacity of more than 500.0 mAh g-1 in the voltage range of 0 to 1.5 V against Li/Li^+ [57, 58]. Recently the batteries companies and the automakersn are focusing on developing hard carbon mainly due to its reversible capacity that has been reported between 200 to 600 mAh g^{-1} [59, 60]. This high capacity of hard carbon is due to the high porosity large surface area and several graphene sheets.

The two-dimensional sheets of sp2 carbon with nanometers (single atom) thickness in the honeycomb structure is called graphene. In 1987, after the discovery of the term graphene, this material has been highly investigated due to several extraordinary properties in several fields like engineering, biological, physical, and chemical sciences [61] The number of properties that makes graphene a very good material for li-ion batteries is high surface area, large values of charge mobility, high electronic conductivity, and good mechanical strength [62, 63]. The capacity of graphene to store lithium is a hot topic. When compared to graphite, which has a storage capacity of 372 mAh g^{-1}, single-layer graphene has a low lithium storage capacity. However, when more graphene layers are utilized, its lithium storage capacity increases from 780.0 mAh g^{-1} to 1116.0 mAh g^{-1}, outperforming graphite [64, 65].

Graphene conjugated with metals, phosphide, and metal oxide could be used as an anode side material for li-ion batteries, according to current lithium-ion battery research. For example, Si-Hwa Lee et al. synthesized Graphene nanotube iron Nanostructure and used as anode in li ion batteries and get specific capacity of 1024 mAh g^{-1} [66]. In another study Jun Yang et al. synthesized cobalt phosphide nanowires decorated on reduced graphene oxide and achived reversible capacity of 960 mAh g^{-1}

over 200 cycles at a current density of 0.2 A g^{-1} [67] SnO_2 is a strong choice for anode material in lithium batteries, but it has a short cyclic life due to volume variations, which affects the batteries' reversible storage capacity [68]

2.1.3 Alloying type Anode Materials

Many types of anode materials that store lithium through by an alloying/de-alloying reaction process. Main advantages of alloy type anode materials is that they have higher specific capacity, high energy density and are safe to use. Common issues with this type of anode are they have large irreversibility capacity, huge capacity fading and poor cycling. Examples of these materials are Silicon (Si), germanium (Ge), tin (Sn), antimony (Sb) etc and Si/Sn based oxides. The specific theoretical capacity of such anodes are very high as compared to intercalation type materials (e.g., theoretical capacity of SnO_2 is 1494 mA h g^{-1} [69] while the capacity of silicon is as high as 4200 mA h g^{-1} [70, 71]. Wang et al. study Ni and Fe combined with Si and achieved first discharge capacity around 1180 mA h g^{-1} [72].

Silicon is the second most abundant element in the earth crust and silicon has both a high volumetric capacity of 9786 mA h cm^{-3} and a gravimetric capacity of 4200 mA h g^{-1} for lithium storage [73]. Moreover, the discharge potential of silicon is also very close to graphite (0.40 V vs Li/Li^+) [74]. Silicon is a very cost-effective and environmentally friendly material that is why it is the most suitable anode material for future research that includes the batteries for hybrid electric automobiles and electric automobiles. The high specific capacity of the silicon is due to the generation of the LiSi binary compound for example $Li_{12}Si_7$, $Li_{13}Si_4$, $Li_{22}Si_5$, and Li_7Si_3. The major drawbacks that limit the use of silicon are the volume expansion during the alloying/de-alloying process (i.e., up to 400%) and the formation of the silicon compounds at the solid electrolyte interface (SEI).

A lot of effort has been made to bypass these issues by working on the nanoscale of silicon. For example X. Zhou and coworkers prepared Si nanoparticles which are intercalated in graphene sheets and showed 1153mAh g^{-1} after 100 cycles [75]. In another other study YunXie et al. synthesized nitrogen doped carbon encapsulating silicon nanoparticles and achieved specific capacity of 1185mAh g^{-1} [76]. The focus of the research is on the morphology of the nanostructured silicon for example nanowires, nanotube, and nanosphere were considered because they can provide the required free space to accommodate Si expansion throughout the alloying/de-alloying process.[77].

These nanostructures show good electronic conductivity and chemical stability but the process for their fabrication is not cost-effective. Therefore, still, these technologies are not applicable at the industrial level. The researchers are working on different synthesis techniques like hydrothermal or solvothermal to up scale the manufacturing of these anode materials for commercial purpose.

The germanium is in to focus of the anode material of Li-ion batteries due to its high lithium storage capability that is 1623 mAh g^{-1} through the alloying and de-alloying process. Germanium has greater electric conductivity than silicon nearly 10^4 times higher [78]. The lithium diffusion into the germanium is 15 times higher than silicon at room temperature and 400 times higher at 360 °C temperature. The high-power output of germanium is very useful for high-power density applications like hybrid electric vehicles and electric vehicles. The drawback for the germanium is the high volume change of nearly 300% during the intercalation and de-intercalation process that limit the use of the germanium as anode material for heavy application [79]. H. Lee and his coworkers embedded Ge nano particles into carbon matrix and achieved specific capacity of 1067 mAh g^{-1} [80].

Similarly, to control the volume change problem there is a need to research germanium with different active anode materials at the nanoscale for the high-end application of the lithium-ion batteries.

2.1.4 Conversion type Anodes

To improve li-ion batteries and their application in large scale power grids. one should require a better understanding of li-ion battery. for example in electric vehicle main interest of researcher is that to investigate such systems which have high voltage redox sites this is done by increasing volumetric capacity to reduce the size of electrodes [81]. To get a higher capacity, one should utilize all potential oxidation states of a compound via conversion reactions in which more than one electron is transferred per transition metal ion, rather than 0.5–1.0 electrons as in intercalation compound [82]. This type of behavior is generally shown by transition metals which include metals oxides, phosphides, selenides, etc. they have high capacity, low cost but main issue with these materials they have poor capacity retention, short cycle life and high cost of production. In this type, there is oxidation and reduction reaction and composition and decomposition of lithium compound. These types of materials generally show the theoretical capacity of 500 to 1000 mA h g^{-1}.

Iron oxide is abundantly present in the earth's crust which makes it cheaper. Iron oxide is non-toxic and environment friendly that's why it is excessively used as anode in Li-ion batteries. Fe_2O_3 and α-Fe_2O_3 show the theoretical capacity of 925 mA h g^{-1} and 1000 mA h g^{-1} respectively [83]. Iron oxide has very low conductivity, iron accumulation during the charge/discharge process, low diffusion of Li-ions, and high-volume expansion makes the cycling performance very low. To overcome these issues there is a huge potential in the field of nanomaterials. Some studies show that the scientific community is working on morphology, size, and porosity also some researchers are working on the reaction kinetics and power densities [84-87]. For example, Wu et al have researched the morphology effect and the size of α-Fe_2O_3 nanorods with and without porosity ranging from 300.0 to 500.0 nm [88].

For rechargeable Li-ion batteries, metal phosphides are heavily discussed. Metal Phosphides can react with lithium under conversion mechanism or intercalation/deintercalation mechanism. This depends upon transition metal and phosphorous bonds under an electrochemical environment. The metal phosphide can be divided into two groups. The first group work on the conversion reaction method. In this type, the bond between the phosphorous and the metal will be broken which results in the lithium phosphides and nanosized metal particles. The second group involves lithium diffusion through the insertion and de-insertion method without breaking the bond of metal phosphorous.

In recent years scientific communities investigating extensively transition metal chalcogenides because they can be good for anode candidates in Li-ion batteries due to their high energy capacity. However, they do not have good cycling stability because electrodes get pulverized during large volume changes occurring in conversion reactions between transition metal chalcogenides and Li-ions. To overcome this issue researchers introduce carbon species that enhance electrical conductivity and accommodate volume changes[89]. For example, Huang and co-workers recently prepared a material in which SnS nanoparticles were decorated on N-doped3D graphene [90] by this they can reduce the pulverization and achieve 87% retention even after 1000 cycles. In another study, Peng et al. anchored cobalt sulfide nanoplates on reduce graphene oxide which shows reversible high capacity after 1000 cycles [91]. Huang et al. prepared an anode V_2S_5 and graphite hybrid which shows 496 mAh g^{-1} after 500 cycles. Hou et al reported cobalt selenides embedded in carbon

matrix which can cycle up to 10 000 cycles [92]. Chen's group reported a microsphere of $FeSe_2$ which shows the stable capacity of 372 mAh g^{-1} after 1000 cycles [93].

Keeping in view of above discussion, the conversion mechanism is still under development and has a lot of potential for researchers. The problem with these types of materials is that they have low specific capacity retention, a short life cycle, and high production costs. These problems can be tackled by employing low-cost binary metal chalcogenides such as aluminum and copper in a carbon matrix. Low-cost metal combinations can help to reduce production costs, and carbon matrices will provide electrode integrity, extending the battery's life cycle.

Chapter 3

Experimental Section

3.1 Synthesis of electrodes materials

3.1.1 Synthesis of Copper MOF

Copper MOF was synthesized by a solvothermal method as illustrated by the schematic shown in Fig 3-1. In short, $Cu(NO_3)_2.3H_2O$ (5 g, 20 mmol) and 1,3,5-Benzene tricarboxylic acid ($C_6H_3(CO_2H)_3$) (2.5 g, 12mmol) were sonicated for 15 min in a solution containing an equal amount of Di-methyl-formamide (DMF), Ethanol and DI water in a beaker. Then this solution was placed in a heating oven at 75^oC for 24 hours. After those particles were collected through centrifugation (at 4000 RPM). In last, particles were washed with DMF 3 times to remove the unreacted species.

Table 1 Materials for the synthesis of Cu MOF

Material Name	**Purity**	**Company Name**
Copper nitrate trihydrate $Cu(NO_3)_2.3H_2O$	99.99%	Sigma
1,3,5-Benzene tricarboxylic acid $C_6H_3(CO_2H)_3$	99.99%	Sigma
Di-methyl-formamide (DMF)	99.99%	Sigma
Ethanol	99.99%	Local
Deionized water	99.99%	Local

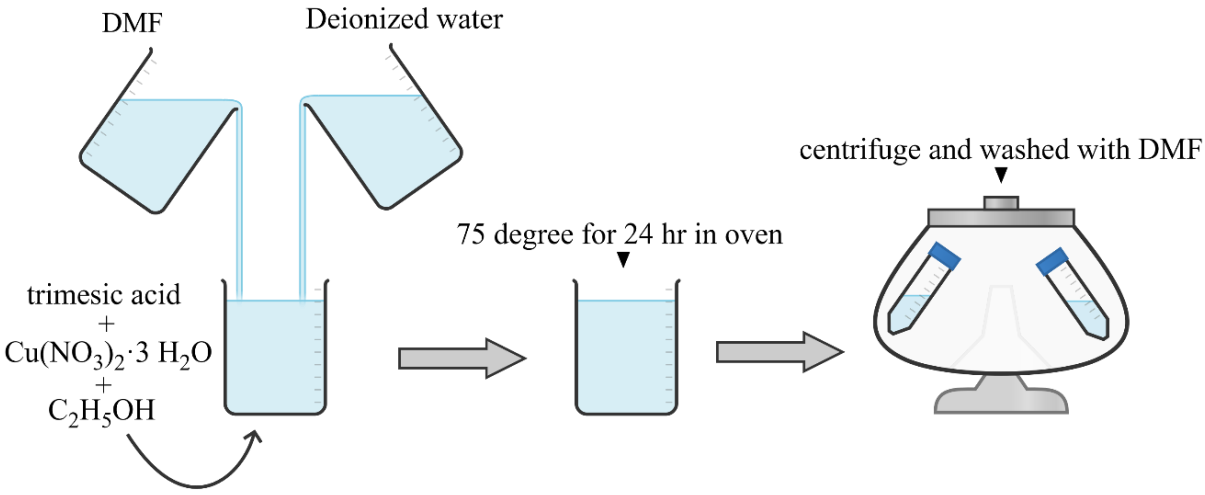

Figure 3-1 Synthesis of Copper MOF

Collected particles were vacuum dried in an oven at room temperature.

3.1.2 Synthesis of Aluminum MOF

Aluminum MOF was synthesized by the solvothermal method as illustrated in Fig 3-2 $Al(NO_3)_3 \cdot 9H_2O$ (1.12 g, 3 mmol) was dissolved in 30ml of Deionized water (solution A). 1,3,5-Benzene tricarboxylic acid (0.63 g, 3 mmol) was dissolved in 30ml of Dimethylformamide (DMF) (Solution B). After that Solution B was mixed with Solution A and stirred for 10 min. This solution was transferred into a 100ml Teflon-lined autoclave and kept at 120^{o}C for 10 hours. Particles were collected through centrifugation at 4000 rpm. After that washed with Dimethylformamide (DMF) and Deionized water 3 times. Particles were dried at 100 for 12hr in a vacuum oven.

Table 2 Materials for the synthesis of Al MOF

Material Name	**Purity**	**Company Name**
Aluminium nitrate nonahydrate $Al(NO_3)_3 \cdot 9H_2O$	99.99%	Sigma
1,3,5-Benzene tricarboxylic acid $C_6H_3(CO_2H)_3$	99.99%	Sigma
Di-methyl-formamide (DMF)	99.99%	Sigma
Deionized water	99.99%	Local

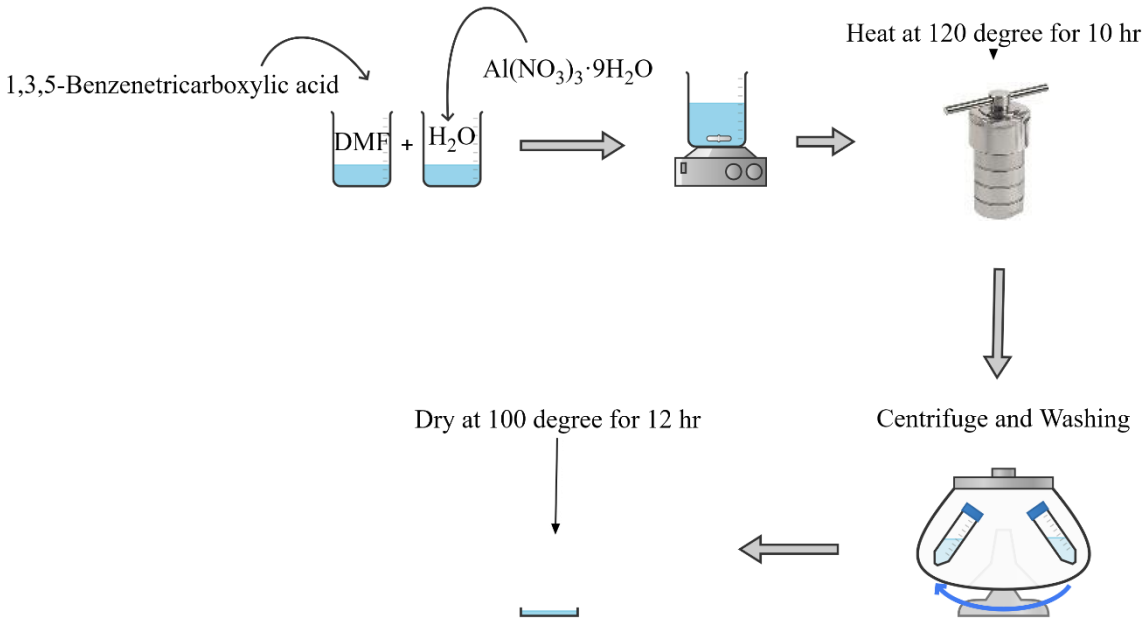

Figure 3-2 Synesis of Al-MOF

3.1.3 Synthesis of Copper-Aluminum MOF

Copper-Aluminum MOF was synthesized by the solvothermal method as illustrated in Fig 3-3. $Al(NO_3)_3 \cdot 9H_2O$ (1.876 g, 5 mmol) and $Cu(NO_3)_2.3H_2O$ (1.208 g, 5 mmol) were dissolved in 30ml of Deionized water (Solution A). $C_6H_3(CO_2H)_3$ (1.261 g, 3 mmol) was dissolved in 30ml of Ethanol (solution B). Solution A was mixed with solution B and stirred for 10 min. Next, the solution was poured into a 100ml Teflon-lined autoclave and maintained at 120^oC for 24 hours. Particles were collected and rinsed in ethanol and deionized water, through centrifugation. In last particles were dried at 100^oC for 12 hours in a vacuum oven.

Table 3 Materials for the synthesis of Al-Cu MOF

Material Name	Purity	Company Name
Aluminum nitrate nonahydrate $Al(NO_3)_3 \cdot 9H_2O$	99.99%	Sigma
Copper nitrate trihydrate $Cu(NO_3)_2.3H_2O$	99.99%	Sigma
1,3,5-Benzene tricarboxylic acid $C_6H_3(CO_2H)_3$	99.99%	Sigma
Ethanol	99.99%	Sigma
Deionized water	99.99%	Local

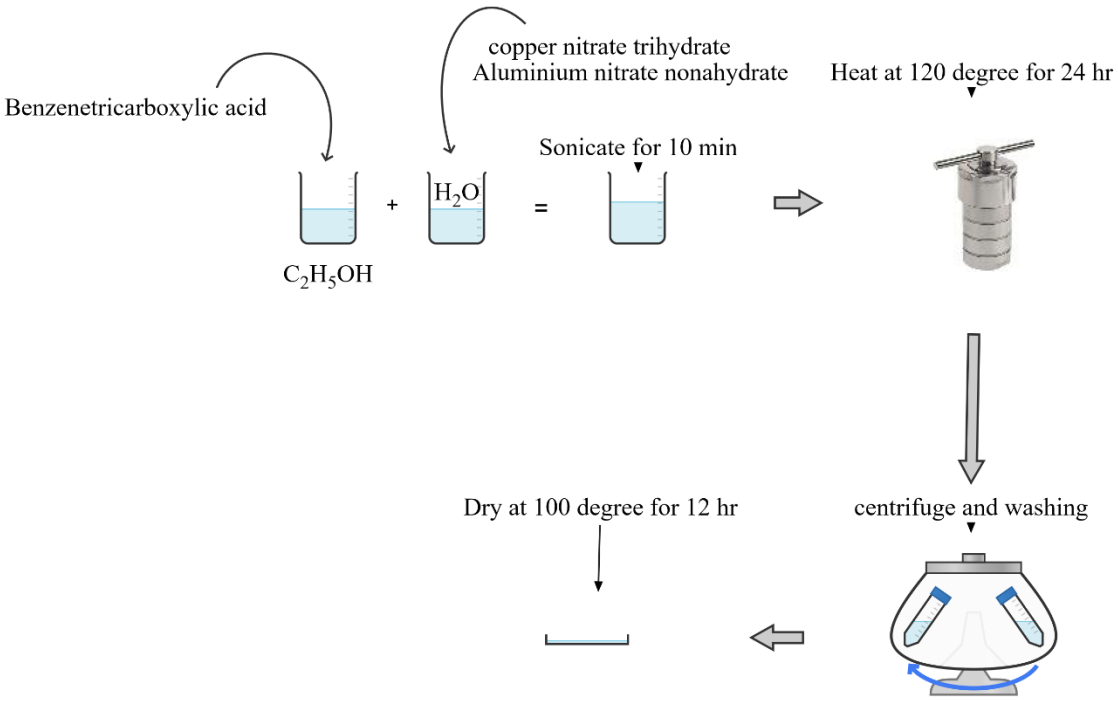

Figure 3-3 synthesis of Al-Cu MOF

3.2 Selenization of electrode materials

All the above-prepared electrode materials were selenized on the condition shown in Fig. Precursor, and well-ground selenium powder (in weight ratio 1:2) was placed at the opposite ends of the boat. The boat was covered with Al-foil, and

selenization was carried out at 300°C for 4 hours with the ramping rate of 5°C/min under the Ar/H_2 (10%vol H_2) environment. Then annealing was carried out at 400°C for 1 hour with the ramping rate of 5°C/min. Finally, the selenized product was cooled down naturally at room temperature.

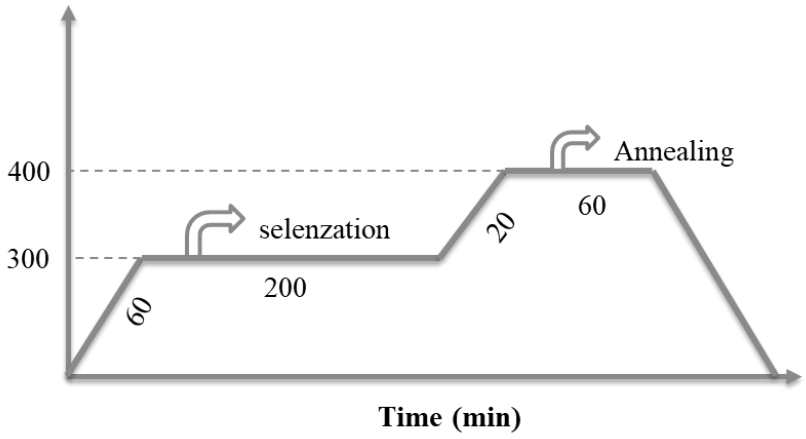

Figure 3-4 condition for selenization

3.3 Preparation of electrode

The working electrode was prepared by mixing active material (Al-Cu-Se), conductive agent (carbon black), and a binding agent (carboxymethylcellulose sodium) in a weight ratio of 75:15:15 respectively. Homogenous slurry (obtained in deionized water) was pasted on well cleaned Cu-foil and dried at 70°C overnight under vacuum.

3.4 Preparation of Lithium half cell

For the preparation of lithium half cell, 2023-type coin cells were fabricated in an Ar-filled glovebox. Prepared electrodes were cut into a small, and for the reference or counter electrode, circular lithium disks were used. To assemble a coin cell, a working electrode was placed at one end of the disc covered by a glass fiber filter paper which is used as a separator so that cell might not get short-circuited circular disk when lithium is placed on top of it, which acts as both reference and counter electrode. On that separator, a few drops of electrolyte (1 M $LiPF_6$ in a (1:1) volume mixture of ethylene carbonate/diethylene carbonate, thus allowing Lithium ions to migrate from one electrode to another. Then the cell was crimped by using a high-pressure crimper, which completely seals the cell's components.

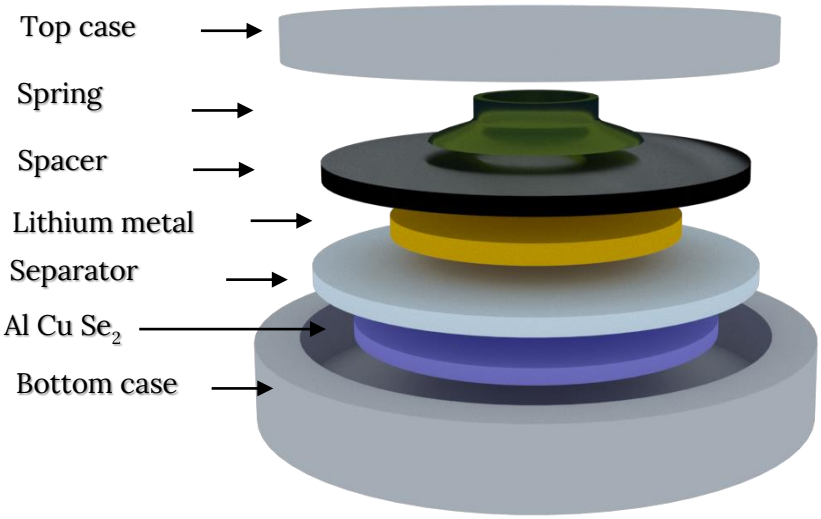

Figure 3-5 Figure schematics for coin cell

Chapter 4

Results and discussions

4.1 Phase structural analysis

4.1.1 XRD analysis of copper selenide

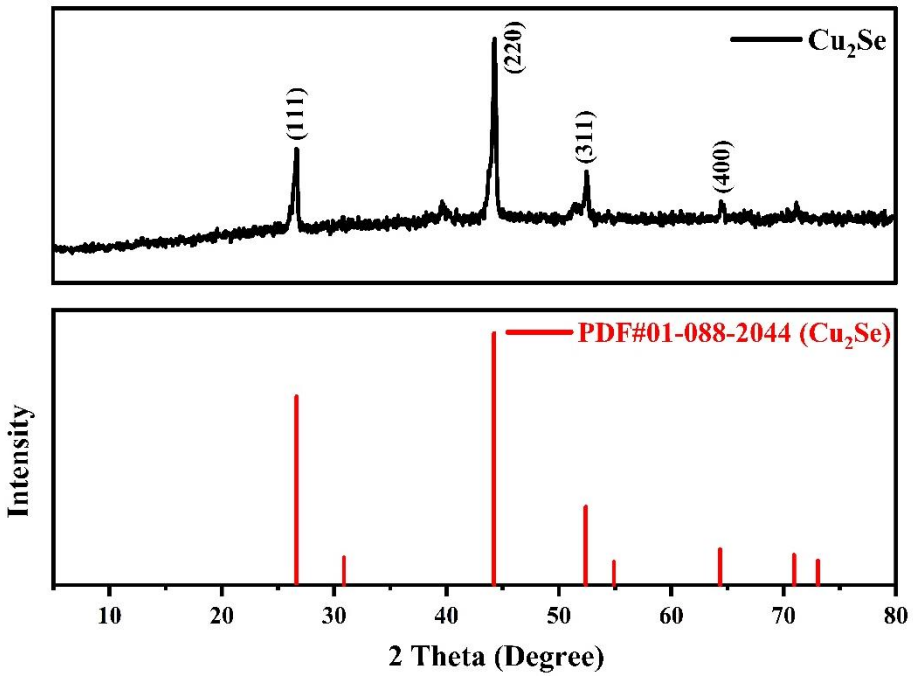

Figure 4-1 XRD analysis of Cu_2Se

XRD was carried out to study synthesized Copper selenide's structural and compositional analysis. The obtained XRD pattern endorsed the formation of a homogeneous cubic structure of Cu_2Se, which is a preliminary agreement with PDF Card # 01-088-2044. There is no peak of impurity observed in the XRD pattern. The maximum X-ray-diffraction was observed along the crystal plan (220) assigned at a diffraction position of $2\theta = 44.234^{O}$. It shows that in this plan, synthesized material is more stable. The other peaks observed as 26.660^{O}, 52.396^{O}, 64.342^{O} corresponds to the plans (111), (311), and (400), respectively.

4.1.2 XRD analysis of Aluminum Selenide

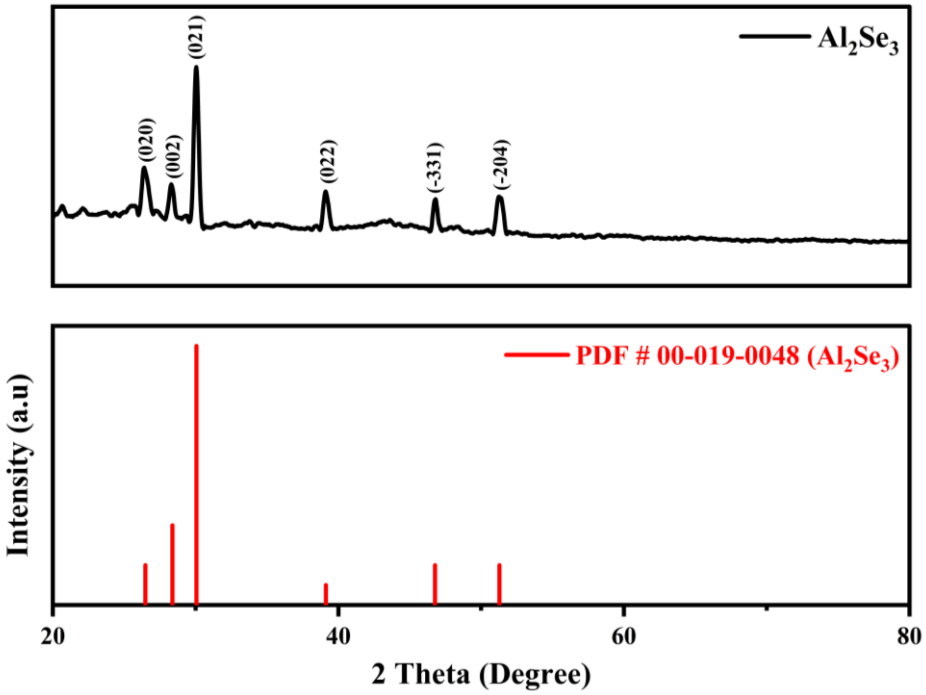

Figure 4-2 XRD analysis of Al_2Se_3

XRD was carried out to study the structural and compositional analysis of synthesized Aluminum selenide. The obtained XRD pattern endorse the formation of a homogeneous Monoclinic structure of Al_2Se_3 which is in complete agreement with PDF Card # 00-019-0048. There is no peak of impurity was observed in the XRD pattern. The maximum X ray-diffraction was observed along the crystal plan (021) assigned at a diffraction position of $2\theta = 30.041^{O}$. It shows that in this plan, synthesized material is more stable. The other peaks observed as 26.240^{O}, 28.249^{O}, 38.979^{O}, 46.760^{O}, 51.092^{O} corresponds to the plans (020), (002), (022), (-331), and (-204) respectively.

4.1.3 XRD analysis of ACSe

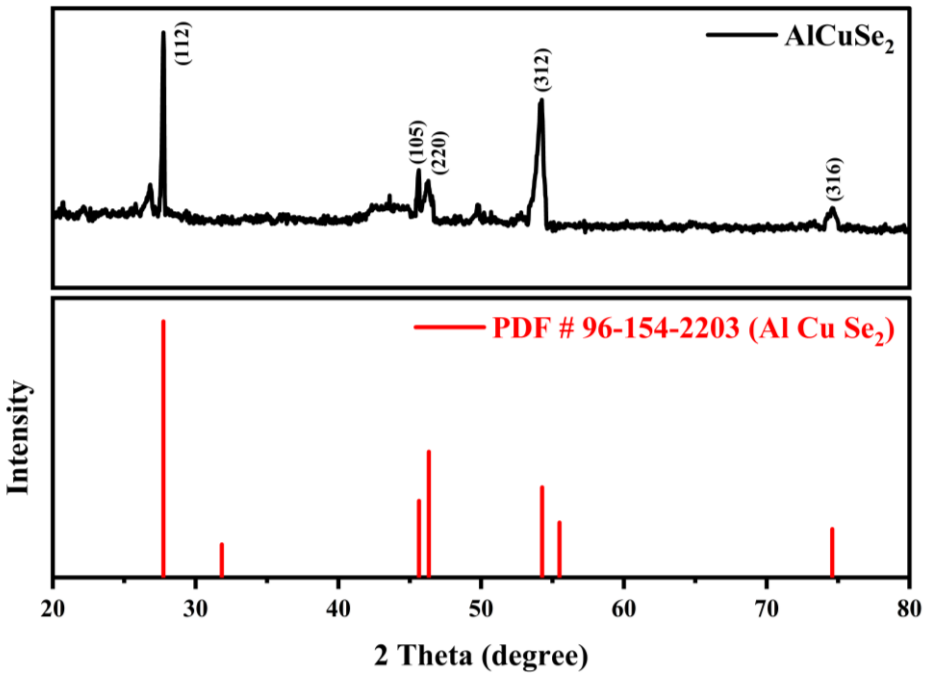

Figure 4-3 XRD graph of Al-Cu-Se

XRD was carried out to study the structural and compositional analysis of synthesized ACSe. The obtained XRD pattern endorsed the formation of a homogeneous tetragonal structure of Al Cu Se_2, which is a preliminary agreement with PDF Card # 96-154-2203. There is no peak of impurity observed in the XRD pattern. The maximum X-diffraction was observed along the crystal plan (112) assigned at the diffraction position of $2\theta = 27.750^{O}$. the other peaks observed as 45.617^{O}, 46.262^{O}, 54.276^{O}, and 74.694^{O} corresponds to the plans (101), (220), (312), and (316) respectively.

4.2 Micro-Structural Analysis

4.2.1 SEM

SEM was performed to study the microstructural analysis of synthesized material. The sample for SEM analysis was made by dispersing our synthesized metal selenides in DI water by ultra-sonication for 5 minutes. Then a drop of dispersion was deposited in an adequately cleaned glass slide. Then the sample was made conducting by gold coating using an ion sputtering system. The images taken by SEM revealed the formation of spheres of metal selenides.

4.2.1.1 Copper Selenide

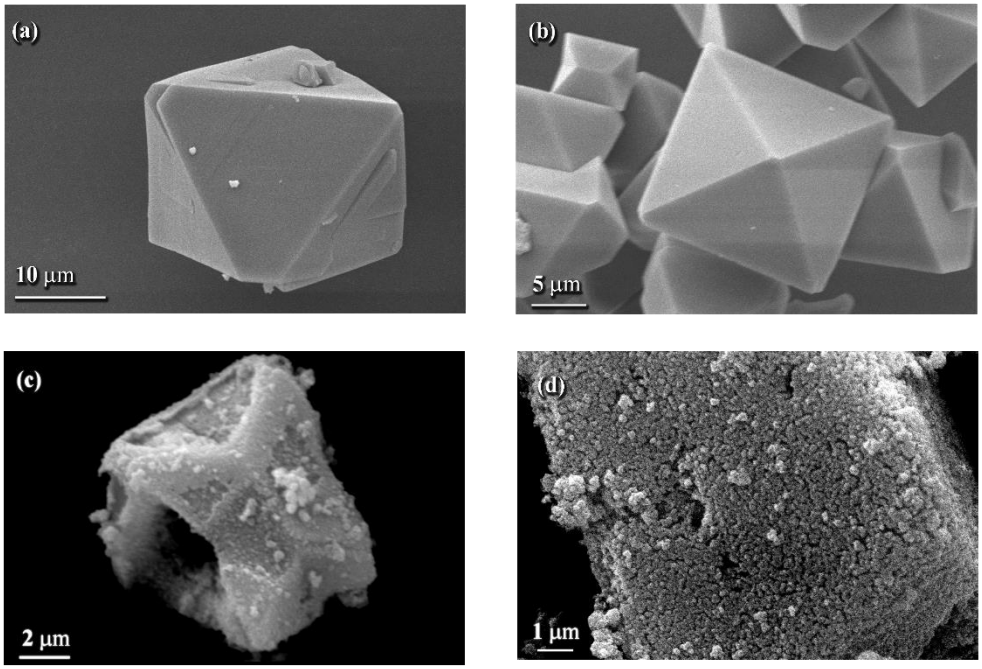

Figure 4-4 SEM (a-b) Cu-MOF (c-d) Cu-Se

Figure (a-b) shows the Copper MOF. From SEM images, it is revealed that Copper MOF has uniform morphology. Figure (c-d) shows the Copper selenide. It is revealed that morphology is almost retained. The carbon matrix encapsulated copper selenide nanoparticles.

4.2.1.2 Aluminum Selenide

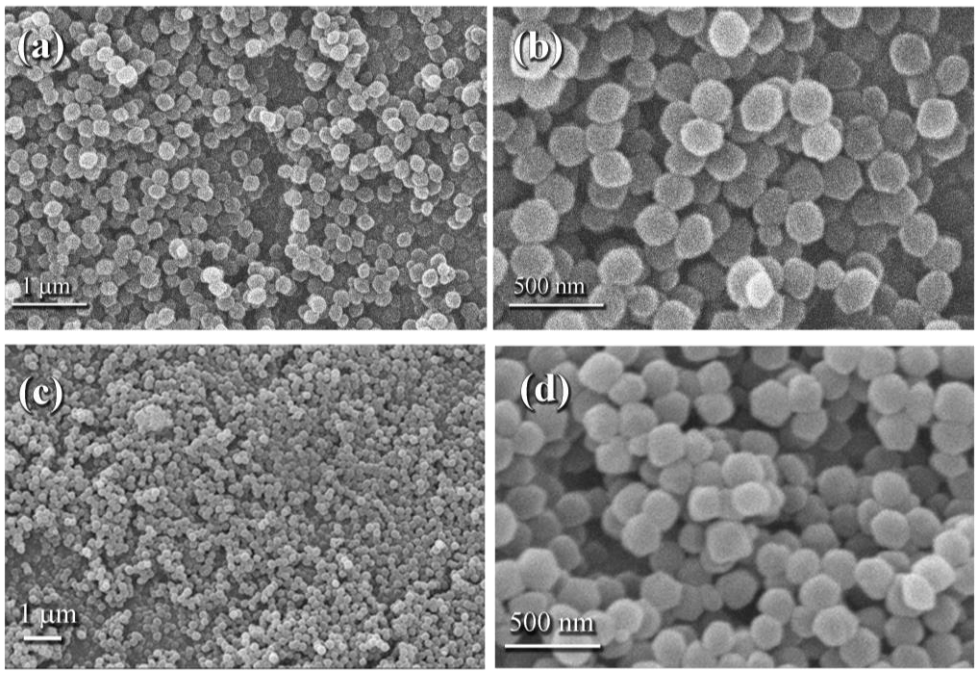

Figure 4-5(a-b) SEM of Al MOF (c-d) SEM of Al-Se

Figure (a-b) shows the Al-MOF. From the images, uniform hexagonal morphology is obtained. Figure (c-d) shows the Al-Se it is also clear that after the selenization, morphology remains intact, and Al-Se is successfully synthesized.

4.2.1.3 Aluminum Copper Selenide

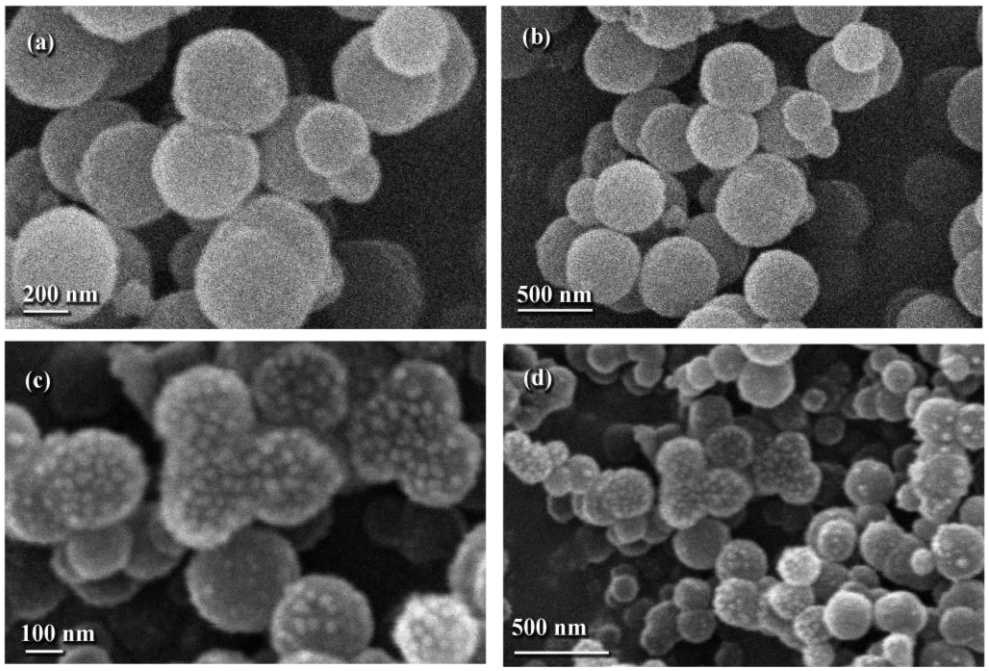

Figure 4-6 SEM of (a-b) Al-Cu-MOF (c-d) Al-Cu-Se

Figure (a-b) shows a binary metal-organic framework with uniform spherical morphology. The average particle size is around 500nm. Figure (c-d) shows binary metal selenides embedded in the carbon matrix. This carbon matrix compensates for the volume changes during the lithiation and de-lithiation process.

4.2.2 EDX

The distribution of elements such as Al, Cu, Se in ACSe was analyzed through EDX elemental mapping analysis in scanning electron microscopy. The EDX maps show the uniform distribution of all elements. Moreover, there is no evidence of stray Se in mapping, which shows complete selenization of Aluminum copper MOF.

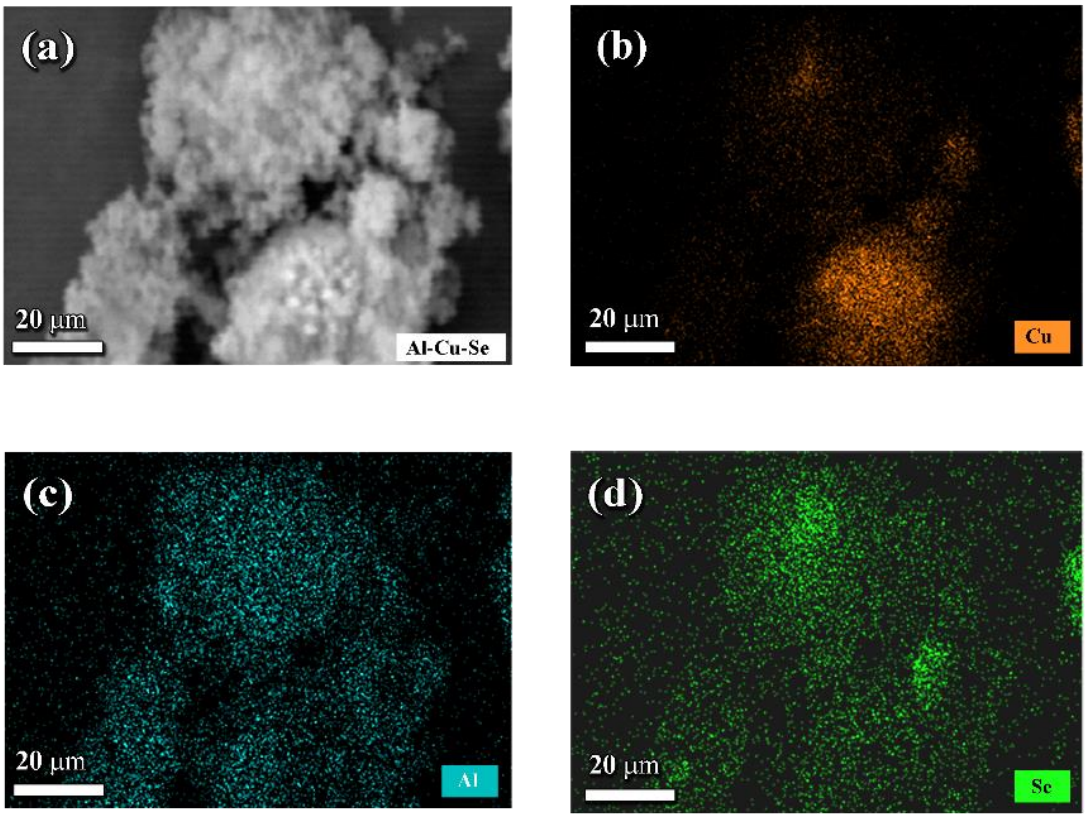

Figure 4-7 EDX Elemental mapping of Al-Cu-Se

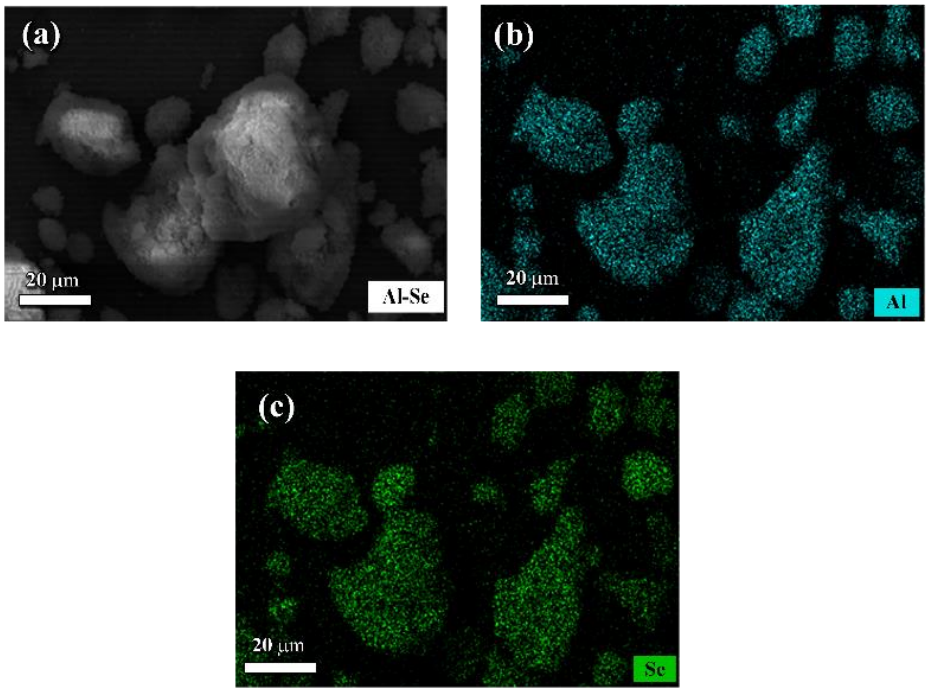

Figure 4-8 EDX Elemental mapping of Al -Se

4.2.3 TEM

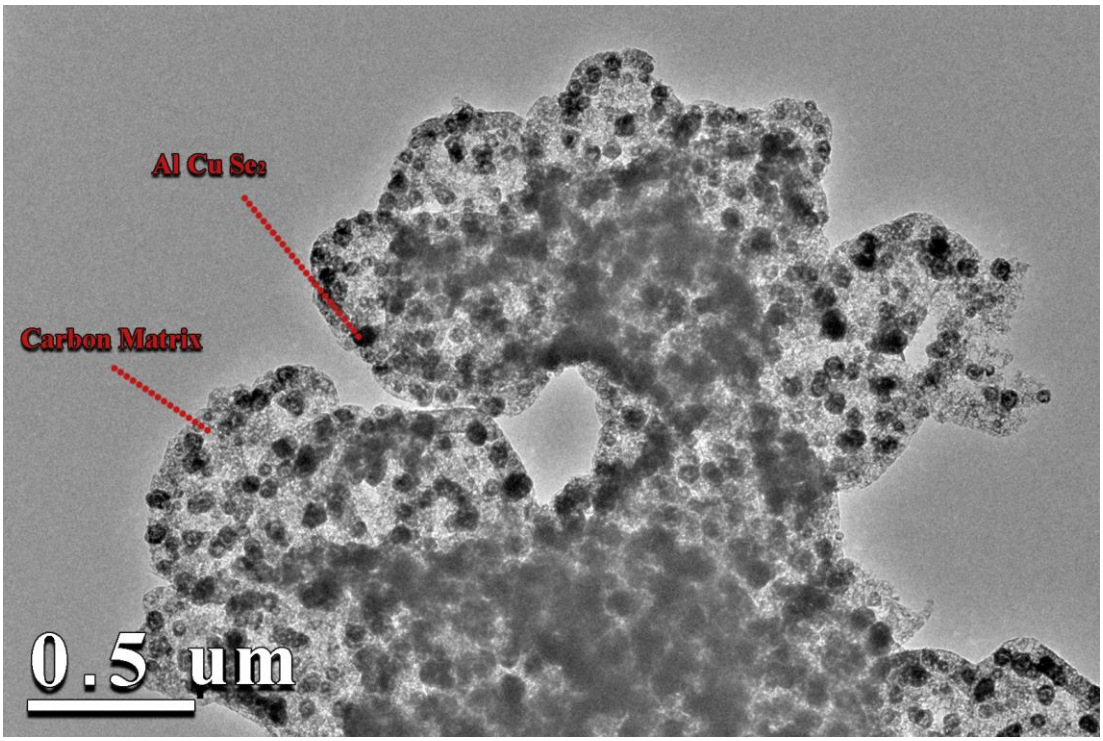

Figure 4-9 TEM of Al-Cu-Se_2

The above figure shows that ACSe embedded in the carbon matrix were successfully synthesized. The figure clearly shows in the background of the carbon structure the stable nano grain formation with very high achieved porosity. Lighter shade shows carbon matrix and darker region shows nano particles. These properties are essential for the electrochemical performance of the anode material of Li-ion batteries. The volume change problem of the electrode material during the lithiation and de-lithiation process is tackled by the nanoscale size of the Al-Cu-Se particles that lower the diffusion length, resulting in minimum volume change. The carbon structure act as a bed to compensate for the volume changes of the material and possible material agglomeration during the charging and discharging process. This analysis confirmed that the binary metal selenide nanoparticles embedded in the carbon matrix were successfully synthesized.

4.2.4 BET

The pore size and surface area are analyzed by BET testing. Isotherm shown in the figure can be categorized as type IV and II. These type of graphs shows the presence of micro and mesopores [94]. ACSe nanosphere shows the Brunauer–Emmett–Teller (BET) surface area of 97.83 $m^2 g^{-1}$. Pore size distribution is calculated

by density functional theory (DFT). It is revealed that the material has micropores of width 0.6 nm. The presence of micro, mesopores and high surface area not only enhance the li^+ ion surface interaction but also increase the electronic conductivity by shortening the ion diffusion length; hence these factors play an essential role in improving the electrochemical properties of the material.

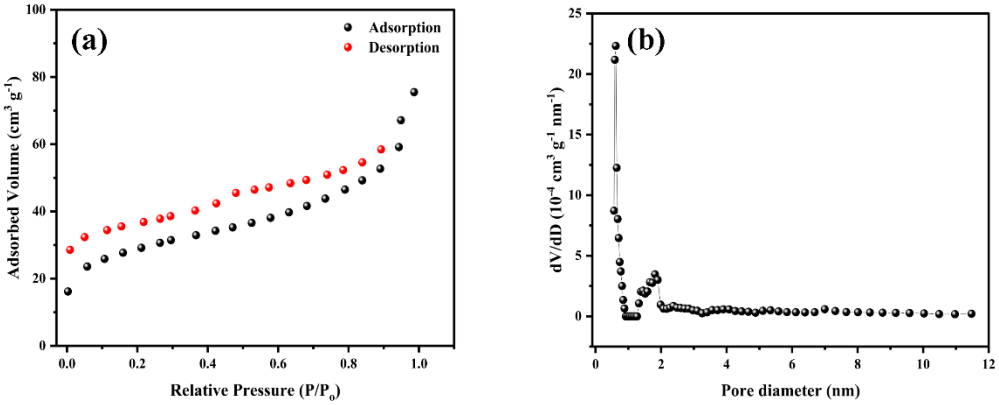

Figure 4-10 (a) N_2 adsorption-desorption isotherms for ACSe (b) Corresponding pore size distribution

4.3 Electrochemical Characterization

4.3.1 Cyclic Voltammetry Analysis

To analyze redox reactions occurring in electrodes, CV was carried out and its result is shown in the figure.

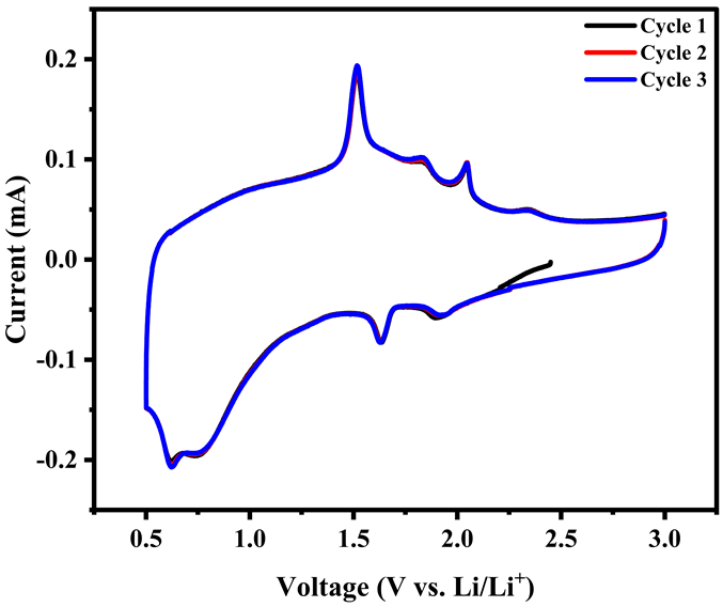

Figure 4-11 CV curves of the Al-Cu-Se anode in lithium half-cells for first three cycles at rate of 0.2 mV S^{-1}

The first three CV curves of ACSe at the scan rate of 0.2 mV s^{-1} reveal various reduction and oxidation peaks in the voltage range of 0.5-3V. The first peak is observed at ~0.62V it can be associated with Li_2Se and nanocrystal of aluminum and copper. The following cycles show more redox peaks at voltage ~0.75, ~1.63V, and ~1.91V. These peaks can be attributed to the transformation of metal selenides to Li_2Se due to the insertion of Li+ ions. The cycles show good overlapping, and the area under each cycle was almost the same, which can be ascribed to reversible and stable cycling performance for anode material.

4.3.1 Galvanostatic Charge/Discharge Analysis

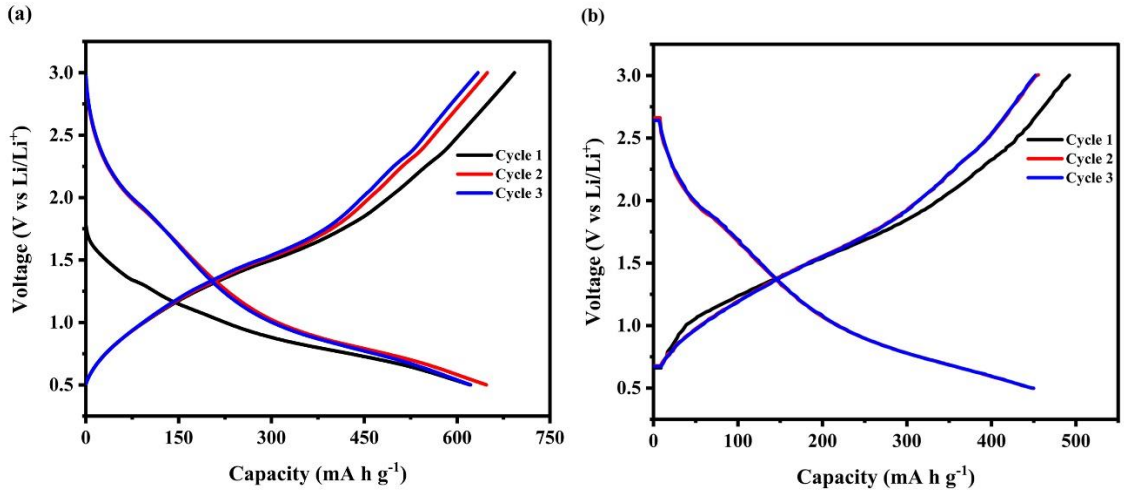

Figure 4-12 Electrochemical discharge and charge profiles (between 0.5 and 3.0 V) of the Al-Cu-Se anode at a current rate of (a) 0.1 A g^{-1} (b) 4 A g^{-1}

figure (a-b) shows first three cycles of charge discharge a of lithium half-cell at 0.1 A g^{-1} and 4 A g^{-1} respectively. Figure (a) show high initial discharge capacity of 692.6 mA h g^{1} of ACSe under the voltage window of 0.5-3V at 0.1 A g^{-1} . The following cycles shows overlapping with the capacity the retention of 693.6 mA h g^{-1}. The capacity loss between the first and succeeding cycles is ~8.51%. figure (b) shows show high initial discharge capacity of 455.5 mA h g^{-1} of ACSe under the volage window of 0.5-3V at high scan rate of 4 A g^{-1}. The following cycles shows overlapping with the capacity retention of 447.7 mA h g^{-1}. The capacity loss between first cycle and the succeeding cycles is ~8.10%. All the observed plateaus in charge/discharge satisfy CV results. The overall good performance of the ACSe is due

to the larger amount of nano porous carbon which leads to the greater surface area and porosity that result in the high storage capacity and better rate capability.

4.3.2 Rate Capability

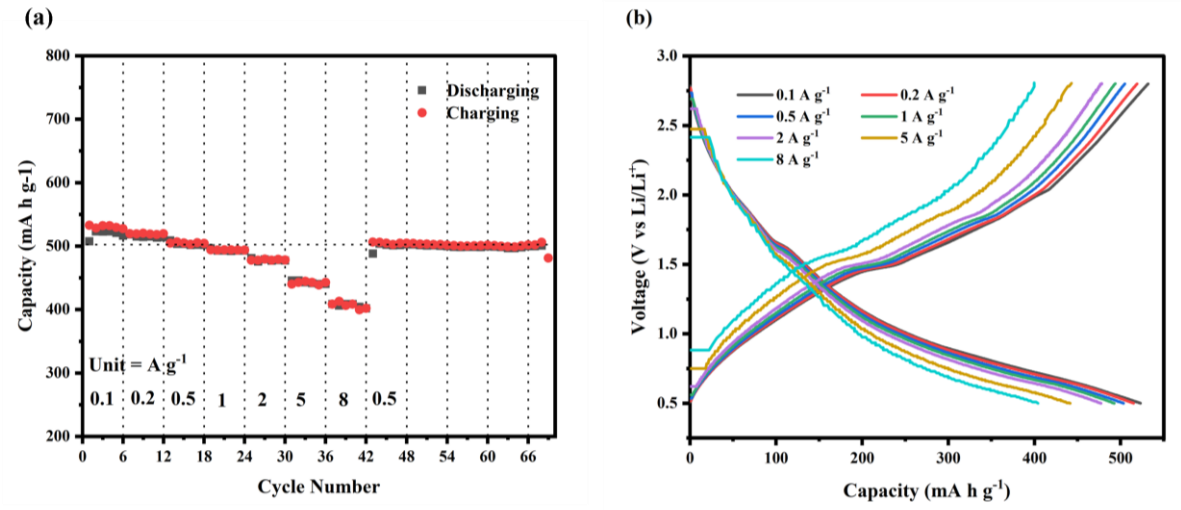

Figure 4-13 (a) Rate performances of Al-Cu-Se at various current densities ranging from 0.1 A g^{-1} to 8 A g^{-1} (b) charge/discharge profiles at corresponding current densities

The capacity retention of synthesized sample was evaluated by charging and discharging of sample material at different current rates as shown in the figure (a). At high current density anode material show excellent performance. ACSe can deliver 401.9 mA h g^{-1} and 442.9 mA h g^{-1} even at high current rates of 5 A g^{-1} and 8 A g^{-1} respectively. When current densities were increased from 0.1 to 0.2, 0.5, 1, 2, 5 and 8 A g^{-1} the specific capacities were 572.2, 519.5, 504.1, 493.8, 478.0, 442.9 and 401.9 mA h g^{-1} respectively and when current rate varied reversely to 0.5 A g^{-1} then the specific capacity was fully recovered to 505.9 mA h g^{-1}. Figure (b) shows the charge/discharge profile of increasing current densities. This also shows that electrode fully recovered specific capacity at 0.5 A g^{-1}.

4.3.3 Cyclic performance

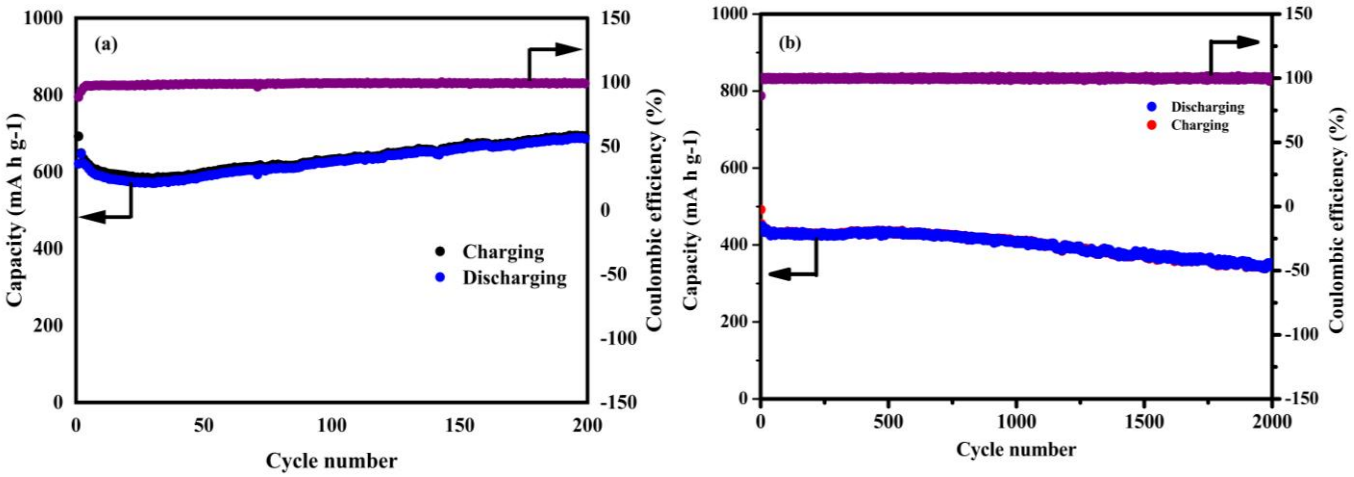

Figure 4-14 comparison of cycling performances of Al-Cu-Se at a current density of (a) 0.1 $A\ g^{-1}$ and (b) 4 $A\ g^{-1}$

Long cyclic performance of ACSe was assessed at 0.1 A g^{-1}(Figure a) and 4 A g^{-1} (Figure b). ACSe show stable and reversible discharge capacity of 692.8 mA h g^{-1} after 200 cycles at current density of 0.1 A g^{-1}. The same anode material was tested at high current density of 4 A g^{-1} for 2000 cycles it is observed that the electrode exhibits a high specific capacity of 351 mA h g^{-1}. With few exemptions the columbic efficiency is between 98-99%.

Conclusion

The unique structure in which aluminium copper selenide was embedded into the carbon matrix helps achieve the stabilized lithium conversion/insertion and deconversion/extraction during the charging and discharging process. The structure was driven from the MOF as precursor formation of selenides through the selenization process. The excellent reversibility and rate capability were achieved during the charging and discharging process as anode material of the Li-ion battery. In attaining the desired electrochemical performance, the uniformity achieved, and structural integrity of the nano porous framework entertained the central part to enhance its performance. The high surface area, morphology, and high porosity that help proper accessibility of lithium-ion towards active sites play a crucial role in achieving reversibility and high-rate capability. This research design development has given the

potential to develop economical, stable, and better anode materials for Li-ion batteries and can take it to large-scale applications with high energy storage demands.

References

1. Peter, S.C., *Reduction of CO2 to Chemicals and Fuels: A Solution to Global Warming and Energy Crisis.* ACS Energy Letters, 2018. **3**(7): p. 1557-1561.
2. Bilgen, S., *Structure and environmental impact of global energy consumption.* Renewable and Sustainable Energy Reviews, 2014. **38**: p. 890-902.
3. Hoegh-Guldberg, O., et al., *The human imperative of stabilizing global climate change at 1.5 C.* Science, 2019. **365**(6459).
4. Lee, H., *Intergovernmental Panel on Climate Change.* 2007.
5. Assi, A.F., A.Z. Isiksal, and T. Tursoy, *Renewable energy consumption, financial development, environmental pollution, and innovations in the ASEAN+ 3 group: Evidence from (P-ARDL) model.* Renewable Energy, 2021. **165**: p. 689-700.
6. Xu, J., et al., *Potassium-based electrochemical energy storage devices: Development status and future prospect.* Energy Storage Materials, 2021. **34**: p. 85-106.
7. Gu, S., et al., *Recycling of mixed lithium-ion battery cathode materials with spent lead-acid battery electrolyte with the assistance of thermodynamic simulations.* Journal of Cleaner Production, 2020. **266**: p. 121827.
8. Rahangdale, D. and A. Kumar, *Acrylamide grafted chitosan based ion imprinted polymer for the recovery of cadmium from nickel-cadmium battery waste.* Journal of Environmental Chemical Engineering, 2018. **6**(2): p. 1828-1839.
9. Xu, X., et al., *A room-temperature sodium–sulfur battery with high capacity and stable cycling performance.* Nature communications, 2018. **9**(1): p. 1-12.
10. Pei, Z., et al., *A Flexible Rechargeable Zinc–Air Battery with Excellent Low-Temperature Adaptability.* Angewandte Chemie, 2020. **132**(12): p. 4823-4829.
11. Jiang, H., et al., *A high power density and long cycle life vanadium redox flow battery.* Energy Storage Materials, 2020. **24**: p. 529-540.
12. Wang, S., et al., *Excellent stability and electrochemical performance of the electrolyte with indium ion for iron–chromium flow battery.* Electrochimica Acta, 2021. **368**: p. 137524.
13. Wu, M., et al., *A zinc–bromine flow battery with improved design of cell structure and electrodes.* Energy Technology, 2018. **6**(2): p. 333-339.
14. Ye, S., et al., *Highly stable single Pt atomic sites anchored on aniline-stacked graphene for hydrogen evolution reaction.* Energy & Environmental Science, 2019. **12**(3): p. 1000-1007.
15. Valøen, L.O. and J.N. Reimers, *Transport properties of LiPF6-based Li-ion battery electrolytes.* Journal of The Electrochemical Society, 2005. **152**(5): p. A882.

16. Xu, X., et al., *Experimental test of properties of KCl–MgCl2 eutectic molten salt for heat transfer and thermal storage fluid in concentrated solar power systems.* Journal of Solar Energy Engineering, 2018. **140**(5).
17. Aydogmus, O., G. Boztas, and R. Celikel, *Design and analysis of a flywheel energy storage system fed by matrix converter as a dynamic voltage restorer.* Energy, 2022. **238**: p. 121687.
18. Cheayb, M., et al., *Modelling and experimental validation of a small-scale trigenerative compressed air energy storage system.* Applied energy, 2019. **239**: p. 1371-1384.
19. Zhang, Y., et al., *Experimental study on the vibrational performance and its physical origins of a prototype reversible pump turbine in the pumped hydro energy storage power station.* Renewable energy, 2019. **130**: p. 667-676.
20. Singh, R., A. Altaee, and S. Gautam, *Nanomaterials in the advancement of hydrogen energy storage.* Heliyon, 2020. **6**(7): p. e04487.
21. Li, W., J. Liu, and D. Zhao, *Mesoporous materials for energy conversion and storage devices.* Nature Reviews Materials, 2016. **1**(6).
22. Lee, J.W., et al., *A Facile and Template-Free Hydrothermal Synthesis of Mn3O4 Nanorods on Graphene Sheets for Supercapacitor Electrodes with Long Cycle Stability.* Chemistry of Materials, 2012. **24**(6): p. 1158-1164.
23. Zhang, L., et al., *A review of supercapacitor modeling, estimation, and applications: A control/management perspective.* Renewable and Sustainable Energy Reviews, 2018. **81**: p. 1868-1878.
24. Kivisaari, J., et al., *Preparation and measurement of air electrodes for alkaline fuel cells.* Journal of power sources, 1990. **32**(3): p. 233-241.
25. De Geeter, E., et al., *Alkaline fuel cells for road traction.* Journal of Power Sources, 1999. **80**(1-2): p. 207-212.
26. Santos, J. and T. Matencio, *Ceramic Materials for Solid Oxide Fuel Cells*. 2011.
27. Kulkarni, A. and S. Giddey, *Materials issues and recent developments in molten carbonate fuel cells.* Journal of Solid State Electrochemistry, 2012. **16**(10): p. 3123-3146.
28. *<qt1767q1zv.pdf>*.
29. Reddy, M.V., et al., *Brief history of early lithium-battery development.* Materials, 2020. **13**(8): p. 1884.
30. Dunkin, M.R., et al., *Improved ionic conductivity and battery function in a lithium iodide solid electrolyte via particle size modification.* Electrochimica Acta, 2021. **388**: p. 138569.

31. Park, H., et al. *Simple and Effective Gas-Phase Doping for Lithium Metal Protection in Lithium Metal Batteries*. in *ECS Meeting Abstracts*. 2018. IOP Publishing.
32. Krause, F.C., et al., *High specific energy lithium primary batteries as power sources for deep space exploration.* Journal of the Electrochemical Society, 2018. **165**(10): p. A2312.
33. Li, X., et al., *Porous graphene nanocages with wrinkled surfaces enhancing electrocatalytic activity of lithium/sulfuryl chloride batteries.* RSC Advances, 2021. **11**(16): p. 9469-9475.
34. *<1.2100445.pdf>*.
35. Reddy, M.V., et al., *Brief History of Early Lithium-Battery Development.* Materials (Basel, Switzerland), 2020. **13**(8): p. 1884.
36. *<0079-6786-2878-2990003-1.pdf>*.
37. Mizushima, K., et al., *LixCoO2 (0<šd1): A new cathode material for batteries of high energy density.* Solid State Ionics, 1981: p. 171-174.
38. Fouassier, C., et al., *Sur de nouveaux bronzes oxygénés de formule NaχCoO2 (χ1). Le système cobalt-oxygène-sodium.* Journal of Solid State Chemistry, 1973. **6**(4): p. 532-537.
39. Goodenough, J.B., K. Mizushima, and P.J. Wiseman, *Electrochemical cell and method of making ion conductors for said cell*. 1984, Google Patents.
40. Sasaki, T., Y. Ukyo, and P. Novák, *Memory effect in a lithium-ion battery.* Nature Materials, 2013. **12**(6): p. 569-575.
41. Lain, M.J., J. Brandon, and E. Kendrick, *Design Strategies for High Power vs. High Energy Lithium Ion Cells.* Batteries, 2019. **5**(4): p. 64.
42. Funke, K., *Solid State Ionics: from Michael Faraday to green energy-the European dimension.* Sci Technol Adv Mater, 2013. **14**(4): p. 043502.
43. Lazzari, M. and B. Scrosati, *A Cyclable Lithium Organic Electrolyte Cell Based on Two Intercalation Electrodes.* Journal of The Electrochemical Society, 2019. **127**(3): p. 773-774.
44. *6 Carbon from waste source for Li-ion battery*, in *Carbon-Based Smart Materials*. 2020. p. 153-180.
45. Shin, J.-H., et al., *Coffee waste-derived one-step synthesis of a composite structure with Ge nanoparticles surrounded by amorphous carbon for Li-ion batteries.* Journal of Alloys and Compounds, 2021. **889**.
46. An, S.J., et al., *The state of understanding of the lithium-ion-battery graphite solid electrolyte interphase (SEI) and its relationship to formation cycling.* Carbon, 2016. **105**: p. 52-76.

47. Vargas, Ó., et al., *Contribution to the Understanding of Capacity Fading in Graphene Nanosheets Acting as an Anode in Full Li-Ion Batteries.* ACS Applied Materials & Interfaces, 2014. **6**(5): p. 3290-3298.
48. Vargas C, O.A., Á. Caballero, and J. Morales, *Can the performance of graphene nanosheets for lithium storage in Li-ion batteries be predicted?* Nanoscale, 2012. **4**(6): p. 2083-2092.
49. Armstrong, A.R., et al., *Lithium-Ion Intercalation into TiO2-B Nanowires.* Advanced Materials, 2005. **17**(7): p. 862-865.
50. Scrosati, B. and J. Garche, *Lithium batteries: Status, prospects and future.* Journal of Power Sources, 2010. **195**(9): p. 2419-2430.
51. Girishkumar, G., et al., *Lithium−Air Battery: Promise and Challenges.* The Journal of Physical Chemistry Letters, 2010. **1**(14): p. 2193-2203.
52. Park, T.-H., et al., *Enhancing the rate performance of graphite anodes through addition of natural graphite/carbon nanofibers in lithium-ion batteries.* Electrochimica Acta, 2013. **93**: p. 236-240.
53. Marom, R., et al., *A review of advanced and practical lithium battery materials.* Journal of Materials Chemistry, 2011. **21**(27).
54. Li, C.-C. and Y.-W. Wang, *Importance of binder compositions to the dispersion and electrochemical properties of water-based LiCoO2 cathodes.* Journal of Power Sources, 2013. **227**: p. 204-210.
55. Haik, O., et al., *On the Thermal Behavior of Lithium Intercalated Graphites.* Journal of The Electrochemical Society, 2011. **158**(8).
56. Boyanov, S., et al., *Nanostructured transition metal phosphide as negative electrode for lithium-ion batteries.* Ionics, 2007. **14**(3): p. 183-190.
57. Ni, J., Y. Huang, and L. Gao, *A high-performance hard carbon for Li-ion batteries and supercapacitors application.* Journal of Power Sources, 2013. **223**: p. 306-311.
58. Li, H., et al., *Research on Advanced Materials for Li-ion Batteries.* Advanced Materials, 2009. **21**(45): p. 4593-4607.
59. Bridges, C.A., et al., *In Situ Observation of Solid Electrolyte Interphase Formation in Ordered Mesoporous Hard Carbon by Small-Angle Neutron Scattering.* The Journal of Physical Chemistry C, 2012. **116**(14): p. 7701-7711.
60. Fujimoto, H., et al., *The anode performance of the hard carbon for the lithium ion battery derived from the oxygen-containing aromatic precursors.* Journal of Power Sources, 2010. **195**(21): p. 7452-7456.
61. Gu, Y., F. Wu, and Y. Wang, *Confined Volume Change in Sn-Co-C Ternary Tube-in-Tube Composites for High-Capacity and Long-Life Lithium Storage.* Advanced Functional Materials, 2013. **23**(7): p. 893-899.

62. Hou, J., et al., *Graphene-based electrochemical energy conversion and storage: fuel cells, supercapacitors and lithium ion batteries.* Phys Chem Chem Phys, 2011. **13**(34): p. 15384-402.
63. Liang, M. and L. Zhi, *Graphene-based electrode materials for rechargeable lithium batteries.* Journal of Materials Chemistry, 2009. **19**(33).
64. Brownson, D.A.C., D.K. Kampouris, and C.E. Banks, *An overview of graphene in energy production and storage applications.* Journal of Power Sources, 2011. **196**(11): p. 4873-4885.
65. Liu, Y., et al., *Feasibility of Lithium Storage on Graphene and Its Derivatives.* J Phys Chem Lett, 2013. **4**(10): p. 1737-42.
66. Lee, S.-H., et al., *Graphene–Nanotube–Iron Hierarchical Nanostructure as Lithium Ion Battery Anode.* ACS Nano, 2013. **7**(5): p. 4242-4251.
67. Yang, J., et al., *Graphene and cobalt phosphide nanowire composite as an anode material for high performance lithium-ion batteries.* Nano Research, 2016. **9**(3): p. 612-621.
68. Hwang, H.J., et al., *Multilayer Graphynes for Lithium Ion Battery Anode.* The Journal of Physical Chemistry C, 2013. **117**(14): p. 6919-6923.
69. Kebede, M.A., *Tin oxide–based anodes for both lithium-ion and sodium-ion batteries.* Current Opinion in Electrochemistry, 2020. **21**: p. 182-187.
70. Zhang, W.-J., *A review of the electrochemical performance of alloy anodes for lithium-ion batteries.* Journal of Power Sources, 2011. **196**(1): p. 13-24.
71. Aricò, A.S., et al., *Nanostructured materials for advanced energy conversion and storage devices.* Nature Materials, 2005. **4**(5): p. 366-377.
72. Wang, G.X., et al., *Innovative nanosize lithium storage alloys with silica as active centre*. Journal of Power Sources, 2000. **88**(2): p. 278-281.
73. Wu, H. and Y. Cui, *Designing nanostructured Si anodes for high energy lithium ion batteries.* Nano Today, 2012. **7**(5): p. 414-429.
74. Ashuri, M., Q. He, and L.L. Shaw, *Silicon as a potential anode material for Li-ion batteries: where size, geometry and structure matter.* Nanoscale, 2016. **8**(1): p. 74-103.
75. Zhou, X., et al., *Facile synthesis of silicon nanoparticles inserted into graphene sheets as improved anode materials for lithium-ion batteries.* Chemical Communications, 2012. **48**(16): p. 2198-2200.
76. Xie, Y., et al., *Nitrogen-doped carbon caging silicon nanoparticles for high performance lithium-ion battery anodes.* Journal of Alloys and Compounds, 2021. **860**: p. 158487.

77. Yamada, Y., et al., *Kinetics of electrochemical insertion and extraction of lithium ion at SiO.* Journal of The Electrochemical Society, 2009. **157**(1): p. A26.
78. Chockla, A.M., et al., *Solution-grown germanium nanowire anodes for lithium-ion batteries.* ACS applied materials & interfaces, 2012. **4**(9): p. 4658-4664.
79. Rudawski, N., et al., *Ion beam-mixed Ge electrodes for high capacity Li rechargeable batteries.* Journal of power sources, 2013. **223**: p. 336-340.
80. Lee, H., et al., *Synthesis and optimization of nanoparticle Ge confined in a carbon matrix for lithium battery anode material.* Journal of the Electrochemical Society, 2007. **154**(4): p. A343.
81. Bhatt, M.D. and J.Y. Lee, *High capacity conversion anodes in Li-ion batteries: A review.* International Journal of Hydrogen Energy, 2019. **44**(21): p. 10852-10905.
82. Nitta, N. and G. Yushin, *High-Capacity Anode Materials for Lithium-Ion Batteries: Choice of Elements and Structures for Active Particles.* Particle & Particle Systems Characterization, 2014. **31**(3): p. 317-336.
83. Xu, J.-S. and Y.-J. Zhu, *Monodisperse Fe3O4 and γ-Fe2O3 magnetic mesoporous microspheres as anode materials for lithium-ion batteries.* ACS applied materials & interfaces, 2012. **4**(9): p. 4752-4757.
84. Mitra, S., et al., *Growth and electrochemical characterization versus lithium of Fe3O4 electrodes made by electrodeposition.* Advanced Functional Materials, 2006. **16**(17): p. 2281-2287.
85. Koo, B., et al., *Hollow iron oxide nanoparticles for application in lithium ion batteries.* Nano letters, 2012. **12**(5): p. 2429-2435.
86. Kang, N., et al., *Nanoparticulate iron oxide tubes from microporous organic nanotubes as stable anode materials for lithium ion batteries.* Angewandte Chemie, 2012. **124**(27): p. 6730-6734.
87. Ma, X.-H., et al., *Facile synthesis of flower-like and yarn-like α-Fe2O3 spherical clusters as anode materials for lithium-ion batteries.* Electrochimica Acta, 2013. **93**: p. 131-136.
88. Wu, C., et al., *Synthesis of hematite (α-Fe2O3) nanorods: diameter-size and shape effects on their applications in magnetism, lithium ion battery, and gas sensors.* The Journal of Physical Chemistry B, 2006. **110**(36): p. 17806-17812.
89. Ali, Z., et al., *Hierarchically Porous Fe2CoSe4 Binary-Metal Selenide for Extraordinary Rate Performance and Durable Anode of Sodium-Ion Batteries.* Advanced Materials, 2018. **30**(36): p. 1802745.
90. Xiong, X., et al., *SnS nanoparticles electrostatically anchored on three-dimensional N-doped graphene as an active and durable anode for sodium-ion batteries.* Energy & Environmental Science, 2017. **10**(8): p. 1757-1763.

91. Peng, S., et al., *Unique cobalt sulfide/reduced graphene oxide composite as an anode for sodium-ion batteries with superior rate capability and long cycling stability.* Small, 2016. **12**(10): p. 1359-1368.
92. Ali, Z., et al., *Cobalt selenide decorated carbon spheres for excellent cycling performance of sodium ion batteries.* Energy Storage Materials, 2018. **13**: p. 19-28.
93. Li, D., et al., *Achieving ultrafast and stable Na-ion storage in FeSe2 nanorods/graphene anodes by controlling the surface oxide.* ACS applied materials & interfaces, 2018. **10**(26): p. 22841-22850.
94. Kumar, K.V., et al., *Characterization of the adsorption site energies and heterogeneous surfaces of porous materials.* Journal of Materials Chemistry A, 2019. **7**(17): p. 10104-10137.